AD_____

Award Number: W81XWH-10-1-0196

TITLE: Exosomal microRNA signatures in the diagnosis and prognosis of ovarian cancer

PRINCIPAL INVESTIGATOR: Douglas D Taylor, PhD

CONTRACTING ORGANIZATION: University of Louisville School of Medicine
Louisville, KY 40292

REPORT DATE: Oct 2013

TYPE OF REPORT: FINAL REPORT

PREPARED FOR: U.S. Army Medical Research and Materiel Command
Fort Detrick, Maryland 21702-5012

REPORT DOCUMENTATION PAGE

Form Approved
OMB No. 0704-0188

1. REPORT DATE	2. REPORT TYPE	3. DATES COVERED
Oct 2013	Final	1 Apr 2010-31 July 2013

4. TITLE AND SUBTITLE
Exosomal microRNA Signatures in the Diagnosis and Prognosis of Ovarian Cancer

5a. CONTRACT NUMBER

5b. GRANT NUMBER
W81XWH-10-1-0196

5c. PROGRAM ELEMENT NUMBER

6. AUTHOR(S)
Douglas D. Taylor, PhD

E-Mail: douglastaylor@exosomes.org

5d. PROJECT NUMBER

5e. TASK NUMBER

5f. WORK UNIT NUMBER

7. PERFORMING ORGANIZATION NAME(S) AND ADDRESS(ES)
University of Louisville
Louisville, KY 40292

8. PERFORMING ORGANIZATION REPORT NUMBER

9. SPONSORING / MONITORING AGENCY NAME(S) AND ADDRESS(ES)
U.S. Army Medical Research and Materiel Command
Fort Detrick, Maryland 21702-5012

10. SPONSOR/MONITOR'S ACRONYM(S)

11. SPONSOR/MONITOR'S REPORT NUMBER(S)

12. DISTRIBUTION / AVAILABILITY STATEMENT
Approved for Public Release; Distribution Unlimited

13. SUPPLEMENTARY NOTES

14. ABSTRACT

Our original goal was to correlate exosomal miRNA profiles within circulating tumor-derived exosomes with cancer diagnosis, characterization of circulating tumor-derived vesicles and development of methodology for their specific isolation were essential for specific analyses of tumor-derived exosomal cargoes. Our discovery of exosomal microRNA in cancer patients focused on miRNAs, previously demonstrated in tumor biopsies or ovarian tumor cells. We have observed that while some miRNAs that are up-regulated with the tumor or also up-regulated in their exosomes, some tumor-up-regulated miRNAs are not up-regulated within exosomes. Further, certain miRNAs down-regulated within the tumor are up-regulated in exosomes. We demonstrate that miRNA signatures derived from ovarian tumor exosomes exhibit some miRNAs that are undetectable within the tumor. These findings demonstrate the highly selective nature of miRNA "packaging." Although the exosomal miRNA signatures for ovarian cancer patients appear to be similar regardless of stage, significant differences among early (Stage I and II) and late stage (Stage III) ovarian cancer were demonstrated: increase expression level and elevated expression of three specific miRNAs within exosomes. Exosomes from ovarian cancer patients were demonstrated to possess elevated levels of RNA, including the presence of specific long-noncoding RNA.

15. SUBJECT TERMS- Exosomes, microRNA, Diagnostic biomarkers, Ovarian Cancer

16. SECURITY CLASSIFICATION OF:			17. LIMITATION OF ABSTRACT	18. NUMBER OF PAGES	19a. NAME OF RESPONSIBLE PERSON
a. REPORT	b. ABSTRACT	c. THIS PAGE			19b. TELEPHONE NUMBER *(include area code)*
U	U	U	UU	47	USAMRMC

TABLE of CONTENTS

INTRODUCTION

Despite progress made in the understanding and treatment of ovarian cancer, it remains the fourth leading cause of cancer-related deaths in women, resulting in more than 25,500 new cases and 15,310 deaths annually in the U.S. [1,2] Most women with ovarian cancer are diagnosed at an advanced stage, with 75% of cases diagnosed with extra-ovarian disease. This late diagnosis may reflect the inaccessibility of the ovaries and the lack of early symptoms.[3] The anatomical location of the ovaries results in minimal interference with vital structures or local irritation, making the diagnosis of ovarian cancer difficult, until regional and distant metastases have occurred.

Although ovarian cancer accounts for only a third of gynecologic cancers, it results in 55% of the deaths from gynecologic malignancies and 6% of all cancer deaths in women.[4,5] Long-term survival has not changed significantly in the last two decades, largely due to inadequacy of diagnostic approaches, which only detects well-established overt cancers. Stage I ovarian cancer can be cured in 90% of cases, while five-year survival for patients with advanced disease (Stage III and IV) is less than 21%. In comparison with other cancers associated with women, 73% of endometrial cancers, 55% of breast cancers and 50% of cervical cancers are diagnosed as Stage I, while only 23% of ovarian cancers are diagnosed at an early stage.[6] Thus, prospects for significant improvement in ovarian cancer survival reside in early diagnosis of disease.

The only biomarker currently approved for ovarian cancer detection is CA125 and its quantitation by ELISA has been the "gold standard" for detection of ovarian cancer, since its introduction in 1983.[7] Assessment of CA125 is typically used in disease management, both for disease detection as well as monitoring for disease recurrence; however, the use of CA125 is limited with regard to early stage cancer detection (sensitivity from 50–60%).[8] CA125 quantitation is only approved for and consistently proven for remission monitoring. CA125 is neither sensitive nor specific for de novo ovarian cancer detection, since it is elevated in >50% of women with stage I disease, although it is elevated in more than 80% of patients with advanced stage ovarian cancer. CA125 has poor specificity, which is shown by its elevation in association with benign and malignant breast and colon disease, peritoneal irritants, and benign gynecologic diseases, among others. Significant effort has been expended in the recent years for identifying potential markers that might substitute or complement CA125 in disease management or ultimately in the design of screening strategies.[9]

To address these problems, new technologies are being investigated. New strategies that facilitate proteomic analysis by dramatically simplifying the pre-analytical sample separation and coupling with mass spectrometry (MS) have been introduced for biomarker discovery research. Surface-enhanced laser desorption/ionization time-of-flight mass spectrometry (SELDI-TOF-MS) has received much attention for its use in resolving proteins in biological specimens by binding to biochemically distinct ProteinChip arrays. In LabCorp's technology, 4 serum proteins are examined by ELISA, while Correlogic Systems and Ciphergen Biosystems use mass spectrometry of 7 specific serum components or general peptide patterns in patient serum to define the presence of cancer. SELDI-TOF-MS profiling has been successfully used to differentiate ovarian, breast, prostate, and liver cancer from controls.[10] SELDI-TOF-MS profiling of serum was significantly better than the current standard serum biomarker CA125 at distinguishing patients with ovarian cancer from those with benign ovarian disease and from healthy controls.[11] Studies have shown that the selection of a combination of multiple proteins resolved by SELDI-TOF-MS may become a potential diagnostic approach. An effective screening test for ovarian cancer needs to achieve a high sensitivity and specificity and currently, different proteomic technologies as well as the computational analytic tools used to discern peaks generate different findings. These initial studies on SELDI-TOF-MS profiling insights are promising, and the concept is reproducible in a series of different backgrounds; however, translating this approach into a routine diagnostic test remains difficult.

Jacobs and Menon calculated that to be an effective screening test, an assay needs to achieve a minimum of 99.6% specificity.[12] To achieve this level of specificity, multiple components of the tumor's

characteristics will need to be incorporated into new diagnostic tests for effective detection because of the multifactorial nature of ovarian cancer. A drawback of mass spectrometry techniques is that some samples of importance may be masked by more abundant proteins in the MS as well as in the analysis of the spectrometric output. Prepurification by a number of techniques such as high-performance liquid chromatography and positive or negative selection through affinity binding can remove particular groups of proteins. The greatest challenge in most current mass spectrometry approaches is the dynamic range rather than sensitivity. While removal of prevalent proteins or peptides can greatly increase the informational content that can be acquired from particular samples, prevalent proteins such as albumin can function as carriers of protein subsets of diagnositic significance. Additional studies with larger samples sizes and careful blinding of the independent validation sets are needed before any consideration of application of this platform for screening for ovarian cancer or any other indication should be considered.

One general characteristic of tumors is their ability to release or shed intact, vesicular portions of the plasma membrane (termed membrane fragments, membrane vesicles, microvesicles or exosomes), which was initially described by us.[13] Exosomes are described as microvesicles containing 5′-nucleotidase activity that are released from neoplastic cell lines. These small vesicles (50-100nm in diameter), which were present inside large multivesicular endosomes, contained transferrin receptors, a marker that is used to follow endocytosis and the recycling of cell-surface proteins, that had been internalized from the plasma membrane.[14,15] The precise mechanisms of exosome release/shedding remain unclear; however, this release is an energy-requiring phenomenon, modulated by extracellular signals. They appear to form by invagination and budding from the limiting membrane of late endosomes, resulting in vesicles that contain cytosol and that expose the extracellular domain of transferrin receptors at their surface. Using electron microscopy, studies have shown fusion profiles of multivesicular endosomes with the plasma membrane, leading to the secretion of the internal vesicles into the extracellular environment. The rate of exosome release is significantly increased in most neoplastic cells and occurs continuously.[16] Increased release of exosomes and their accumulation appear to be important in the malignant transformation process. In addition to cancer cells, the release of exosomes was also demonstrated to be associated with cells of embryonic origin (such as the placenta) and activated lymphoid cells.[17-20] Although extracellular shedding of exosomes occurs in other types of cells, under specific physiological conditions, the accumulation of exosomes from non-neoplastic cells is rarely observed, in vivo.[17,21] In contrast, exosomes released by tumor cells accumulate in biologic fluids, including in sera, ascites, and pleural fluids. Exosome release and its accumulation appear to be important features of the malignant transformation. Shed tumor derived exosomes do not mirror the general composition of the plasma membrane of the originating tumor cell, but represent ‘micromaps,’ with enhanced expression of tumor antigens.[17,22]

The release of exosomes appears to be important features of intercellular communication. Since released exosomes express molecules with biologic activity (such as Fas ligand, PD-1, MICA/B, mdr1, MMPs, CD44, and autoreactive antigens),[23-26] the ability of these microvesicles to modulate lymphocyte and monocyte functions have been analyzed in several models. It has been theorized that these released exosomes modulate lymphocyte functions by mimicking “activation induced cell death” (AICD).[27,28] Lymphoid cells appear to release exosomes following activation and these appear to play an essential role in immunoregulation, by preventing excessive immune responses and the development of autoimmunity.[30] It was postulated that exosome release by tumor cells is a re-expression of the fetal cell exosomes and that both constituted pathways to circumvent immunosurveillance.[30]

miRNAs are small endogenous noncoding RNA gene products about 22 nucleotides (nt) long that regulate gene expression in a sequence-specific manner and are found in diverse organisms. With >300 already identified, the human genome may contain up to 1,000 miRNAs. miRNA play key roles in regulating the translation and degradation of messenger RNAs through base pairing to partially complementary sites, predominately in the untranslated region of the message.[31-33] miRNAs are expressed as long precursor RNAs. Drosha, an RNase III endonuclease, is responsible for processing

primary miRNAs in the nucleus and releasing ~70nt precursor miRNAs.[34,35] Drosha associates with the dsRNA-binding protein DGCR8 in human to form the microprocessor complex. Precursor miRNAs are transported to the cytoplasm by exportin-5 and cleaved by the RNase III endonuclease Dicer, releasing 17–24nt mature dsmiRNA.[36,37] One strand of the miRNA duplex is subsequently incorporated into the effector complex RNA-induced silencing complex (RISC) that mediates target gene expression. Argonaute2, a key component of RISC, may function as an endonuclease that cleaves target mRNAs.

While the biological functions of most miRNAs are not yet fully understood, it has been suggested that the miRNAs are involved in various biological processes, including cell proliferation, cell death, stress resistance, and fat metabolism, through the regulation of gene expression.[38] As potential clinical diagnostic tools miRNAs have been shown to be important and accurate determinants for many if not all cancers.[39] Increasing evidence shows that expression of miRNA genes is deregulated in human cancer. The expression of miRNAs is highly specific for tissues and developmental stages and has allowed recently for molecular classification of tumors. To date, all tumors analysed by miRNA profiling have shown significantly different miRNA profiles compared with normal cells from the same tissue. Flow-cytometric miRNA profiling demonstrated that miRNA-expression profiles classify human cancers according to the developmental lineage and differentiation state of the tumors. Specific over- or underexpression has been shown to correlate with particular tumor types. miRNA overexpression could result in down-regulation of tumor suppressor genes, whereas their underexpression could lead to oncogene up-regulation. Using large-scale microarray analysis, cancer cells showed distinct miRNA profiles compared with normal cells with 36 of the 228 miRNA genes overexpressed and 21 downregulated in cancer cells versus normal cells.[40] Hierarchical clustering analyses showed that this miRNA signature enabled the tumour samples to be grouped on the basis of their tissue of origin. Genome-wide profiling studies have been performed on various cancer types, including CLL,[41] breast cancer,[42] glioblastoma,[43] thyroid papillary carcinoma,[44] hepatocellular carcinoma,[45] ovarian cancer,[46] colon cancer,[47] and endocrine pancreatic tumours.[48] In a study of 104 matched pairs of primary cancerous and non-cancerous ovarian tissue, 43 differentially expressed miRNAs were observed; 28 were downregulated and 15 were overexpressed in tumors.[49]

Statistical analyses of microarray data obtained by two different methods, significance analysis of microarrays (SAM) and prediction analysis of microarrays (PAM) from six solid tumours (ovarian, breast, colon, gastric and prostate carcinomas and endocrine pancreatic tumours), demonstrated a common signature composed of 21 miRNAs differentially expressed in at least three tumor types.[50] At the top of the list were miR-21, which was overexpressed in six types of cancer cells, and miR-17-5p and miR-191, which were overexpressed in five. As the embryological origin of the analysed tumors was different, the significance of such findings could be that these common miRNAs participate in fundamental signalling pathways altered in many types of tumor. Supporting the function of these genes in tumorigenesis, it was found that the predicted targets for the differentially expressed miRNAs are significantly enriched for those that target known tumor suppressors and oncogenes.[51] Furthermore, miR-21, the only miRNA overexpressed in all six types of cancer analyzed was shown to directly target the tumor suppressor PTEN, which encodes a phosphatase inhibiting growth and/or survival pathways. The function of PTEN is altered in advanced tumors of various types, including breast, ovarian, gastric and prostate.[52]

KEY RESEARCH ACCOMPLISHMENTS

Over the past 3-year funding period, these investigations have generated multiple accomplishments leading to significant improvements of ovarian cancer diagnostic and prognostic markers.

1. Quantitative and quality characterization of circulating vesicles in ovarian cancer patients
2. Development of methodology for specific isolation of tumor-derived circulating exosomes
3. Expanded analyses of tumor-derived exosomal microRNA expression
4. Demonstration of selective release of specific microRNAs within the tumor exosomes
5. Association of specific microRNAs with the presence of late stage ovarian cancer
6. Discovery of tumor-derived exosomal long-noncoding RNA
7. Expanded quantitation and characterization of circulating vesicles in ovarian cancer patients
8. Development of asymmetric field flow fractionation from isolation of ovarian tumor exosomes.
9. Next generation sequencing analysis of tumor-derived exosomal RNA
10. Exosomal miRNAs linked with other solid tumors
11. Exosomes and their cargoes associated with non-solid tumors
12. Defined the actions of tumor-derived exosomes on target cells

As the original Aim 1 was to define the utility of exosomal miRNA profiles as diagnostic biomarkers by correlating specific miRNAs associated with circulating tumor-derived exosomes with diagnosis (stage and grade), achievement of Items 1 and 2 were essential to enable the specific analyses of tumor-derived exosomes and their contents from those exosomes derived from normal cells within the peripheral circulation (ie, reduction of "noise" to enhance the signal to noise ratio). We have continued to increase the number of ovarian cancer patients at each stage evaluated to define the microRNA signatures of the tumors (Item 3). Our original discovery of exosomal microRNA in cancer patients focused on a small number of miRNAs that previous groups demonstrated to be diagnostic using tumor biopsies or cultured ovarian tumor cells; however, we have observed that while some miRNAs that are up-regulated with the tumor or also up-regulated in their exosomes, some tumor-up-regulated miRNAs are not up-regulated within exosomes (Item 4). In addition, we observed that certain miRNAs that exhibit down-regulation within the tumor are up-regulated in exosomes. We have further investigated this finding and demonstrate that in many cases, miRNA signatures derived from ovarian tumor cell exosomes exhibit some miRNAs that are undetectable within the tumor. Our findings in multiple ovarian tumor cell lines demonstrate commonality in these miRNAs. This finding is in addition to cellular down-regulated miRNAs being up-regulated in exosomes derived from the same cells. These findings demonstrate the highly selective nature of miRNA "packaging" into exosomes. Based on these findings, previous data are being re-evaluated to incorporate those miRNAs (not appearing in the tumor cells) into the "diagnostic" signature. Although the exosomal miRNA signatures for ovarian cancer patients appear to be similar regardless of stage, work within the past 12 months has demonstrated significant differences among early (Stage I and II) and late stage (Stage III) ovarian cancer: general increase expression level and the elevated expression of three specific miRNAs within exosomes (Item 5).

While not included with the original objectives of this study, our work demonstrated that exosomes from ovarian cancer patients possessed elevated levels of RNA (less 400 nt). Our proposal focused on the miRNA populations. However, during the past 12 months, we further analyzed this "larger" RNA material. We demonstrated the presence of specific long-noncoding RNA (Item 6).

Summaries of the findings for these six key research accomplishments are presented on the following pages.

REPORTABLE OUTCOMES

NUMERATION AND CHARACTERIZATION OF CIRCULATING VESICLES IN OVARIAN CANCER

Circulating vesicle concentration and size distribution by Nanoparticle Tracking analysis (NTA): To define the total numbers of circulating vesicles and their size distribution in clinical specimens, unfractionated sera from ovarian cancer patients, patients with benign disease disease and female controls were diluted in PBS (1:50-1:100) and applied directly to the sample chamber of the Nanosight LM10 (Figure 1). Patients with ovarian cancer exhibited an approximately 4-fold increase in the level of total circulating vesicles. The size distribution of these unfractionated vesicles from cancer patients ranged from approximately 50 to 300nm in diameter. Patients with benign disease and controls exhibited a similar size range; however, they possessed a greater percentage of vesicles within the 200-300nm range (versus cancer).

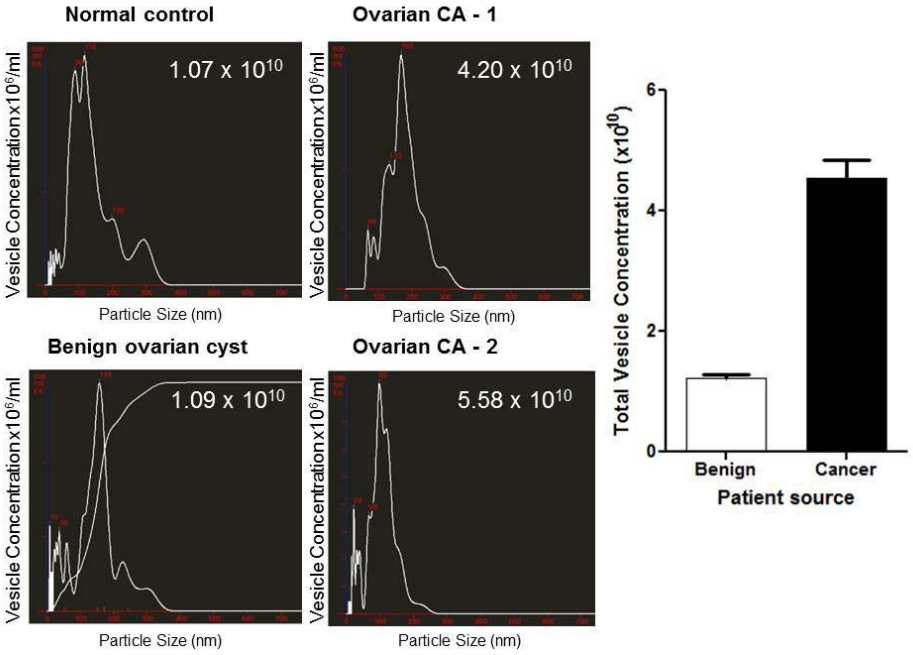

Figure 1: NTA profile of unfractionated circulating vesicles in representative analyses of normal female controls, patients with benign ovarian disease and patients with ovarian cancer. Sera were diluted in PBS and analyzed using a Nanosight LM10. Inset values represent the total number of vesicles counted/ml. The bar graph presents the mean and standard deviation of the vesicles concentrations for patients with benign and malignant ovarian disease.

Size and phenotype characterization of chromatographically isolated vesicles: Over the past 30 years, we have developed and refined an isolation procedure combining differential centrifugation and size exclusion chromatography. The use of high exclusion limit agarose-based gel has been previously demonstrated to generate a vesicle population consistent with those derived from the more labor-intensive sucrose density gradient centrifugation followed by ultracentrifugation. Fractionation of sera on Sepharose 2B resulted in two primary peaks of material (Figure 2A): a void volume and a retained peak. The void volume consists of material exhibiting a molecular weight greater than 50 million Daltons. The individual fractions of the void volume were examined by the Nanosight LM10 and NTA software. Fractions 15, 16, and 17 contained the peak of the void volume. NTA demonstrated a very narrow size range of vesicles (Figure 2B). Fraction 15 contained vesicles ranging from 50-200nm with a primary peak at 94nm (mode = 94nm, mean = 108, SD = 30nm). Fraction 16 exhibited vesicles also ranging from 50-200nm, but the primary peak appeared at 89nm (mode = 89nm, mean = 95nm, SD = 32nm). Fraction 17 consisted on vesicles ranging from 50-200nm with two principal vesicle peaks at 84nm and 108nm (mode =84, mean = 109, SD =30). The majority of the vesicles within Fractions 15, 16, and 17 falls within the 50-100 size range previously described for exosomes.

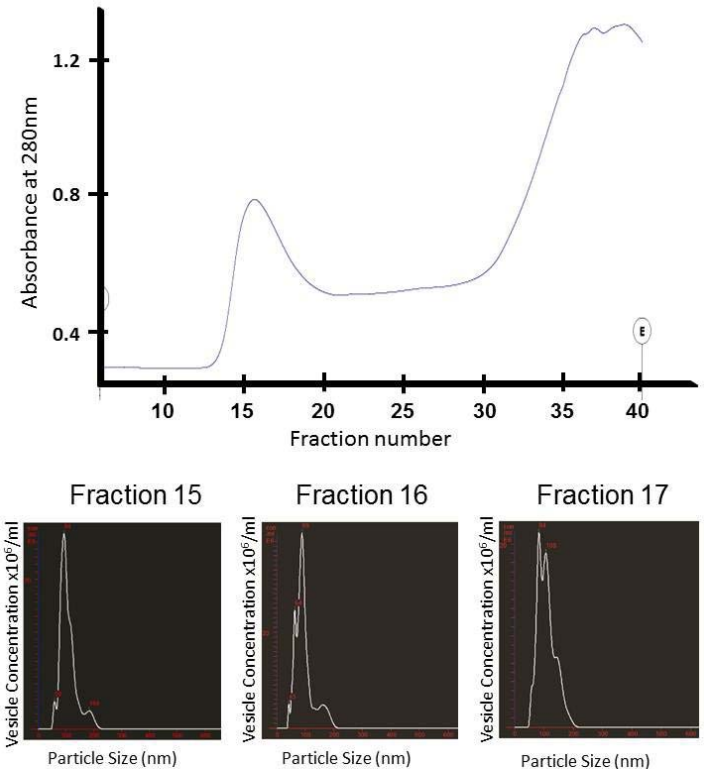

Figure 2: Chromatographic isolation of circulating extracellular vesicles. Panel A: A representative chromatogram of a serum sample obtained from ovarian cancer patient TB08-36 fractionated using a 2% agarose-based size exclusion gel. The peak containing exosomes appears in the void volume. **Panel B:** The three fractions corresponding to the void volume of the column were diluted in PBS and analyzed by NTA using a Nanosight LM10.

Western immunoblotting of chromatographic isolated vesicles: To identify the general distribution of proteins within the vesicular fractions, SDS-PAGE of each chromatographic fraction visualized by protein staining confirmed the similarly of the protein make-up of fractions 15, 16, and 17 (Figure 3A). Western immunoblotting of the individual fractions for specific markers claimed to be associated with either exosomes or microvesicles (Figure 3B). The tetraspanin, CD63, is defined as specific for exosomes, while CD154 (CD40 ligand) has been defined as specific for microvesicles. Western immunoblot analysis of the individual chromatographic fractions demonstrated the co-expressions of CD63 and CD154. While additional later fractions exhibiting elevated levels of CD40L, the void volume peak fractions exhibit the same profile for both CD63 and CD40L. The mutant EGFRvIII, generally considered to be associated with the plasma membrane of cancer cells also appeared to be associated with these void volume vesicles. Thus, while these vesicles are within the classic size range of exosomes, they exhibit markers previously defined as markers of exosomes and microvesicles [14]. Further, the presence of EGFRvIII demonstrates the tumor origin of these vesicles [27]. Similar analyses of vesicles from patients with benign ovarian disease demonstrated CD63-positive vesicles, but the absence of EGFRvIII (Figure 3C).

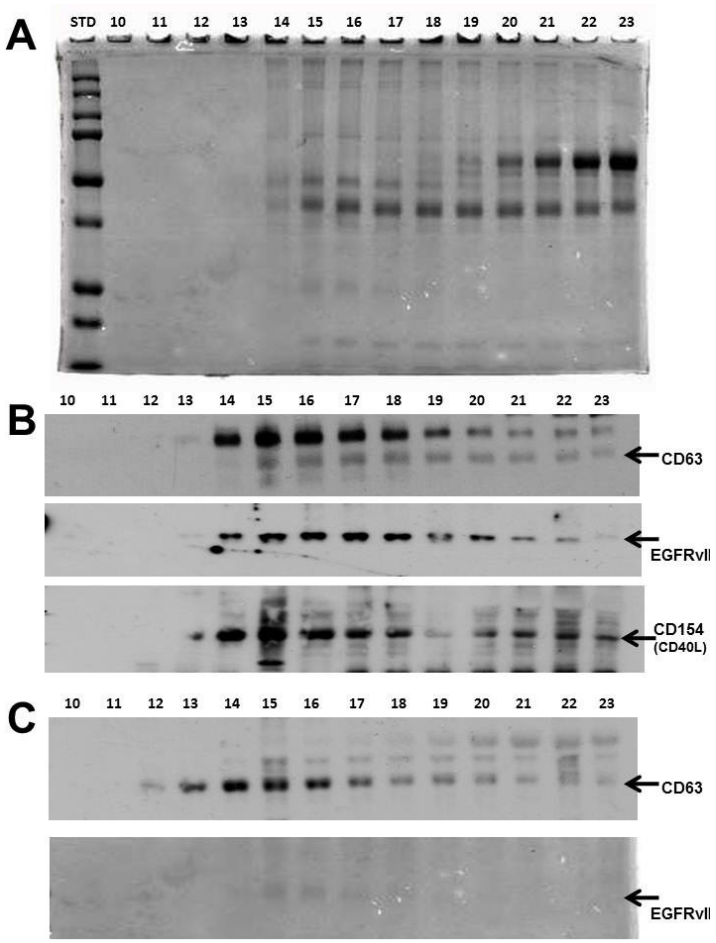

Figure 3: Electrophoretic analyses of the chromatographic fractions from ovarian cancer patient TB08-36 and patient with benign adenoma. Panel A: The separation of proteins from the chromatographic fraction on SDS-PAGE followed by total protein staining with Imperial Purple. Imperial purple stained 10% **SDS-PAGE analysis of a comparable amount of proteins (25µg). Panel B:** Western immunoblot evaluation of published markers of exosomes (CD63), microvesicles (CD154) and tumor origin (EGFRvIII) in vesicles isolated from patient TB08-36. **Panel C:** Western immunoblot evaluation of published markers of exosomes (CD63) and tumor origin (EGFRvIII) in vesicles isolated from patient with benign disease. Chromatographically derived vesicles (25µg protein) were separated on a 10% SDS-PAGE, transferred to nitrocellulose membranes, incubated with anti-CD63, anti-CD154, or anti-EGFRvIII antibodies.

Comparison of sizing methodologies (NTA, SPA, DLS versus EM): NTA, submicron analysis (SPA) and dynamic light scattering were compared with electron microscopic analysis of vesicles. For electron microscopy, the size distribution of vesicles was determined by measuring their diameters directly from electron micrographs of ultracentrifuge pellets (Figure 4A). NTA gave a vesicle size distribution from 50 to 175 nm with a mean = 100nm, mode = 87 and SD = 28 (Figure 4B). Analysis of the same vesicle preparation by DLS indicated a mean diameter of 125.3 ± 1.9nm (Figure 4C), while the submicron particle analysis indicated a range of 80 to 120nm (Figure 4D). These data are further summarized in Table 1. Although the area of the electron microscopy image selected contains vesicles between 50-100nm, EM has been shown to underestimate the size of vesicles. Further, vesicles larger than 100nm are clearly visible in multiple EM fields and the real size distribution of the entire vesicle population is not assessable. Thus, vesicle size ranges defined by EM tend to be subjective. DLS and SPA, while providing an objective size distribution of the entire vesicle population, do not define the concentration of the vesicles.

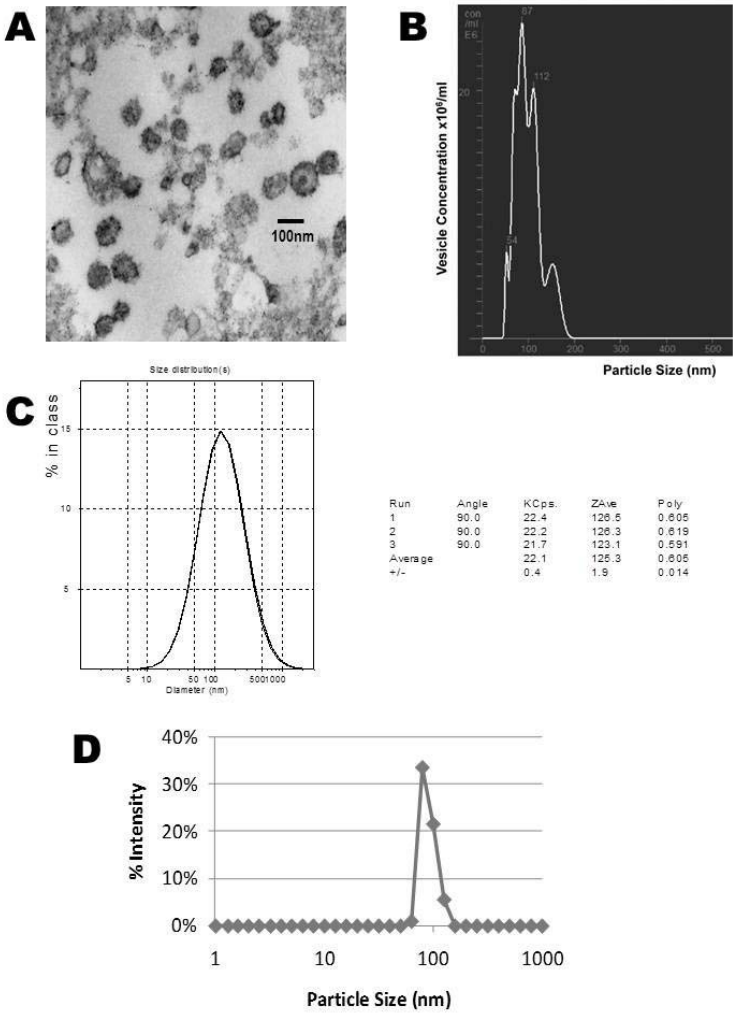

Figure 4: Comparison of vesicle analyses by electron microscopy (A), NTA (B), DLS (C) and submicron particle analysis (D). EM images reveal the presence of nano-sized vesicles with a circular shape. Scale bar, 100 nm (original magnification ×45K).

Phenotype of cell-derived vesicles: A major limitation of DLS and SPA, as well as standard NTA, is that while they can objectively define the vesicle size range, they cannot define the "phenotype" of these vesicles. Using the NanoSight LM10 equipped with the 405-nm blue-violet laser and more sensitive camera to detect fluorescent particles, quantum dots attached to antibodies can be used identify specific subsets of vesicles. The instrument was initially calibrated using 100nm and 200nm fluorescent beads, which can be easily discriminated. Antibodies reactive with either CD63 (exosomes marker) or EpCAM (marker of vesicles derived from epithelial tumors) were conjugated with quantum dots. The labeled vesicle samples were analyzed on the NanoSight LM10, first in light scatter mode and then in fluorescence mode. Figure 5, Panel A shows the NTA profile in light scatter mode and then fluorescence for CD63 (Panel B) and EpCAM (Panel C). The size ranges of the CD63-labeled vesicles are similar, with peaks in the region of 100nm and 180nm whether measured in light scatter or fluorescence mode. The presence of EpCAM on the various size ranges of vesicles indicates their tumor origin. Vesicles both larger and smaller than 100nm exhibit CD63, the marker for exosomes, thus the published definition of exosomes as ranging only from 50-100nm may not be accurate.

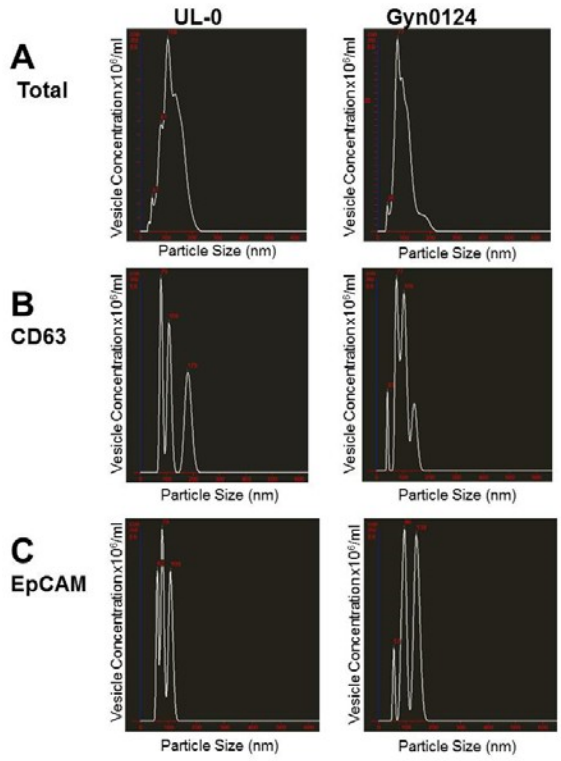

Figure 5: Combination of NTA and fluorescent antibodies to characterize the phenotypes of chromatographically isolated vesicles from two ovarian cancer patients. Vesicle suspensions were incubated with either Qdot-labeled anti-CD63 or Odot-labeled antiEpCAM. These vesicles were then examined in light scattering mode to define total vesicle size distribution (**Panel A**) or in fluorescence mode to define CD63-positive vesicles (**Panel B**) or EpCAM-positive vesicles (**Panel C).**

Analysis of disrupted cell-derived vesicles: Vesicles were chromatographically isolated from ovarian cancer patients and diluted 1:100 in PBS. The sample presented in Figure 6A was the NTA total of untreated vesicles, while Panel B presents the same sample treated with 0.5% Triton X100 for 5 minutes at room temperature and reanalyzed under the same conditions. Based on NTA, the total number of particles was diminished approximately 10-fold. Particle size analysis was further performed using Coulter Model N4 Plus particle size analyzer in PBS at room temperature (SDP analysis, 17 bins in the range from 1-1000nm at 90 degrees) using weight analysis. The sample in Figure 6C presents the SPA distribution of the same sample. The values observed ranged from 80-120nm. Panel D was the same sample treated with 1% Tween 20 for 5 minutes at room temperature and reanalyzed in the same conditions. Based on SPA, the apparent weight average size of the particles shifted from 100 to ~10 nm (range 5-20 nm).

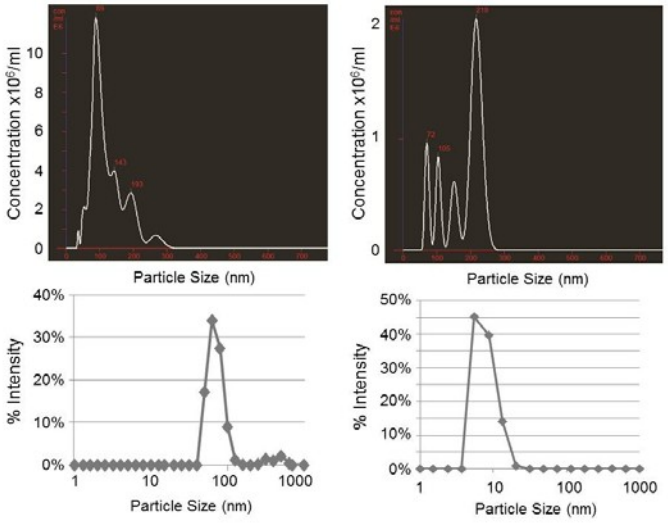

Figure 6: Disruption of light scattering defined particles by non-ionic detergents. The size distributions of chromatographically isolated vesicles were analyzed by either NTA (**A**) or submicron particle analysis (**C**). The same vesicles suspension was treated with either 0.5% Triton X-100 (**B**) or 1% Tween 20 (**D**) for 5 minutes at room temperature and re-analyzed. Treatment with non-ionic detergents disrupted the vesicles, either reducing the number and size under NTA or producing a size shift by SPA.

IMPROVED EXOSOME ISOLATION (IMMUNOTYPING)

While immune cell functions are impaired in most ovarian cancer patients, as defined by the failure to eradicate the tumor, studies suggest immune recognition of tumor antigens remains intact, based on the presence of tumor-reactive IgG, including patients with melanoma, lung, breast, head and neck and ovarian cancers. Malignant diseases are associated with the induction of humoral immunity that is characterized by the generation of reactive IgG against a wide range of tumor-associated antigens (Th2 response). Genetic analyses of tumor cells derived from ovarian cancer patients have demonstrated alterations (mutations or amplifications) in specific genes, including oncogenes, tumor suppressor genes, and proliferation-associated genes. Studies in our laboratory, as well from other groups, have demonstrated a link between cancer-altered genes and development of reactive IgG against their protein products. The actual role of circulating tumor-reactive IgG is unclear; however, they have been demonstrated to correlate with poor prognosis and survival. While the use of tumor-reactive IgG as a potential diagnostic and/or prognostic tool has been investigated over the past decade, to date this work has primarily identified components with shared expression in non-neoplastic tissue and has failed to define antigenic targets exhibiting ubiquitous expression in cancers. These limitations result, in large part, from the use of wild-type recombinant proteins or products of tumor-derived genes translated in non-mammalian cells as targets to define immunoreactivity. The power of utilizing the autologous humoral response is its ability to define both major (mutations, splice variants) and minor alterations (overexpression, altered post-translational processing), which might lead to either altered antigenic appearance or aberrant association with other cellular components resulting in the induction of humoral responses. While the mechanisms underlying the induction of a humoral response appears to be multifaceted: alterations (mutations and post-translational modifications), overexpression, ectopic expression, subcellular compartment translocations, splice variant products, or errors in proteolytic processing of certain proteins have been demonstrated to elicit immune responses in cancer patients. Autoantibody responses to antigens broadly expressed in normal and cancer tissues appears to be attributable to tumor-specific mutations or post-translational modifications.

We hypothesize that by selectively capturing tumor-derived exosomes in blood samples, we can determine in real time the phenotypic state of tumors in individual patients. Cell derived vesicles can be released from many cell types; however, their accumulation within the peripheral circulation appears to be elevated 3-4-fold in cancer patients; however, only a fraction of these are produced by the tumor. Exosomes can be isolated from the peripheral circulation of these patients by high exclusion agarose chromatography. Sera samples (1ml) were separated on Sepharose 2B, monitoring elution at 280nm. The void volume fractions were pooled and added to the upper chamber of a Protein G spin column. The pooled vesicle fraction was incubated with the Protein G gel for 30 minutes at room temperature. The spin column was then centrifuged for 10 seconds at 800rpm and the flow-through collected. The Protein G spin column was washed with 1ml of TBS and re-centrifuged. This flow-through was combined with the first. The Protein G-spin column was then acidified by addition of 0.5ml 0.1M glycine-HCl, pH 2.5. The mixture was incubated for 20 minutes at 4°C and then centrifuged at 800rpm. After centrifugation, the lower chamber contained circulating exosomes isolated based on bound IgG. The eluted exosomes fraction was analyzed quantitatively and qualitatively.

Based on this immunoaffinity approach, we have demonstrated that tumor-derived exosomes are released into the blood and are present at ~2-5 x10^{10}/ml in the peripheral circulation of ovarian cancer patients. We have also demonstrated that exosomal protein profiles from tumor-derived plasma exosomes contain approximate representations of the proteome of the original tumor cell. This vesicular material from cancer patients was examined using a Nanosight LM10 instrument to confirm their size distribution. Isolation of tumor-specific exosomes by our immunoaffinity method based on Protein G beads revealed a subpopulation of vesicles.

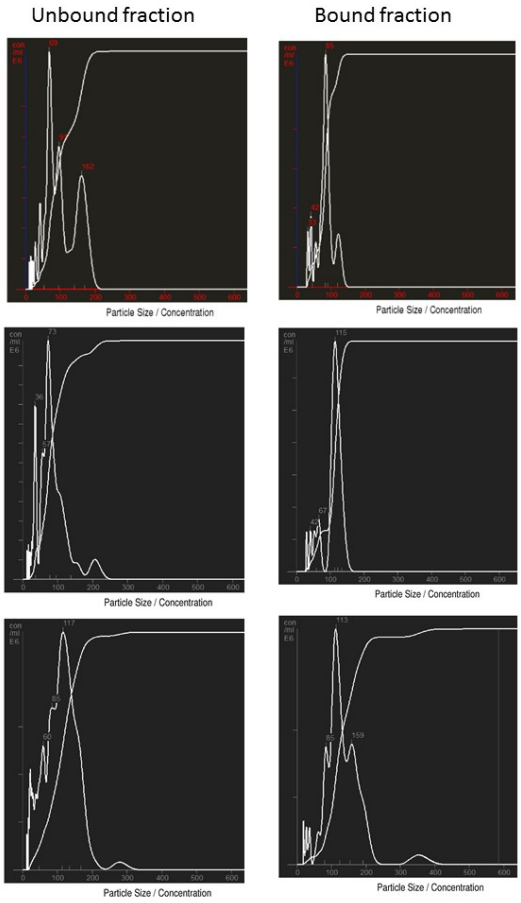

Figure 7: Nanosight tracking profile of sera derived vesicles from ovarian cancer patients. Chromatographically isolated vesicles were incubated with immobilized Protein G. The vesicle fraction not binding to the Protein G is shown as "UNBOUND." The Protein G-binding vesicles were eluted with 0.1M glycine-HCl, neutralized with Tris base and are presented as "Bound."

Isolation of tumor-specific exosomes by our proprietary immunoaffinity method based on Protein G beads revealed a subpopulation with the peak at 72nm. After separation based on Protein G binding, the bound exosomes were eluted and the number of bound vesicular particles was also determined by the

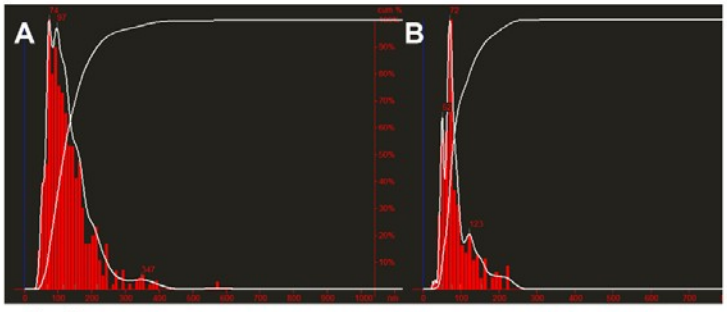

Size distribution of circulating tumor derived exosomes from ovarian cancer ascites defined by the Nanosight LM10. Panel A presents the distribution of total circulating vesicular populations. Panel B presents the distribution of vesicular population by isolated from the circulating vesicles demonstrating the separation of a specific subpopulations.

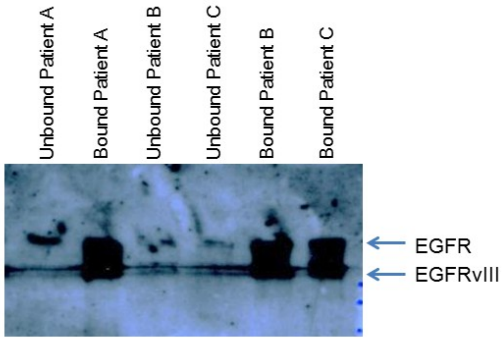

Enrichment of tumor-specific marker, EGFRvIII, based on selection by autoreactive IgG

Nanosight analysis, demonstrating the presence of 2.46 x 10^{10} vesicles/ml. The enrichment of a tumor-specific vesicle population was confirmed by the enhanced expression of the tumor marker, EGFRvIII (defined by Western immunoblotting).

ASSOCIATION AND SELECTIVITY OF MIRNA IN CIRCULATING TUMOR EXOSOMES

Initially, miRNA was isolated from circulating tumor-derived exosomes using mirVana isolation kit. This total small RNA fraction was utilized for miRNA profiling as defined by qRT-PCR microarray analysis. Initial analyses were performed by cancer-specific arrays from SABiosciences. The small RNA-enriched fraction was extracted from the isolated exosomes. Using specific primers, presence and expression level of mature miRNAs was analyzed by TaqMan miRNA Assay (Applied Biosystems) under conditions defined by the supplier. LMW RNA was isolated from exosomes isolated from 1ml of sera using the mirVana miRNA Extraction Kit and quantified by the RiboGreen kit. Single-stranded cDNA will be synthesized from 5.5ng of total RNA in 15µl reaction volume by using the TaqMan MicroRNA Reverse Transcription Kit (AB). The reactions will be incubated first at 16°C for 30 min and then at 42°C for 30 min. The reactions will be inactivated by incubation at 85°C for 5 min. Each cDNA generated will be amplified by quantitative PCR by using sequence-specific primers from the TaqMan microRNA Assays Human Panel on a Agilent M3005P. The 20µl PCR mix will include 10µl of 2× Universal PCR Master Mix, 2µl of each 10× TaqMan MicroRNA Assay Mix and 1.5µl of reverse transcription (RT) product. The reactions will be incubated at 95°C for 10 min, followed by 40 cycles of 95°C for 15 s and 60°C for 1 min. The threshold cycle (C_T) is defined as the fractional cycle number at which the fluorescence passes the fixed threshold (0.2). All signals with C_T ≥37.9 will be manually set to undetermined. The relative quantity (RQ) of the target miRNAs will be estimated by the ΔC_T study by using as reference (exogenous control) for each preparation. Each sample will be run in duplicate and each PCR experiment will include two non-template control wells. From this analyses, exosomal miRNAs that were previously reported to be specifically up-regulated in ovarian cancer cells were examined (Figure 10). Similarly, those exosomal miRNAs shown to be specifically down-regulated were examined.

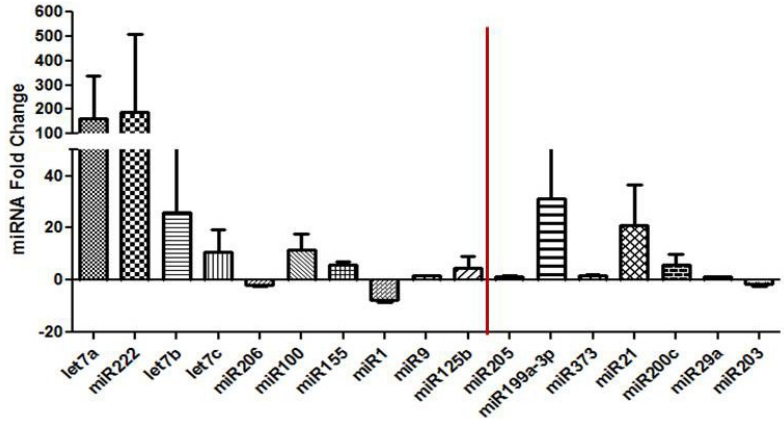

Figure 10: Presence of specific miRNA in tumor derived exosomes (versus normal controls). miRNAs shown to the left of the red line have been demonstrated to be down-regulated in ovarian tumor cells while miRNAs to the right of the red line have been shown to be up-regulated in ovarian cancer.

Within the Cancer qRT-PCR miRNA array, 10 miRNAs have been reported to be up-regulated. Of these, 8 miRNAs were also up-regulated by more than 2-fold within exosomes; however, 2 miRNAs (miR-206 and miR-1) were down-regulated in tumor-derived exosomes. Within the Cancer miRNA qRT-PCR array, 7 miRNAs have been reported to be down-regulated in ovarian tumor cells. Of these 7 miRNAs, only 1 expressed a down-regulation of more than 2-fold (miR-203). Six of these miRNAs were up-regulated by more than 2-fold within exosomes and the other 6 exhibited greater than a 2-fold elevation. These results suggest that certain specific miRNAs are "packaged" within exosomes, with little detectable miRNAs remaining within the originating cells. In contract, miRNAs up-regulated within the tumor cells appear to be mirrored by their expression within the exosomes.

Association of specific microRNAs with the presence of late stage ovarian cancer

One objective of this study was to define miRNA signatures that might differentiate early and late stage ovarian cancer. For these studies, serum specimens of patients with Stage I, II or III serous papillary adenocarcinoma of the ovary were evaluated. The small RNA-enriched fraction was extracted from the isolated exosomes. Using specific primers, presence and expression level of mature miRNAs was

analyzed by TaqMan miRNA Assay (Applied Biosystems) under conditions defined by the supplier. LMW RNA was isolated from exosomes isolated from 1ml of sera using the mirVana miRNA Extraction Kit and quantified by the RiboGreen kit. Single-stranded cDNA will be synthesized from 5.5ng of total RNA in 15µl reaction volume by using the TaqMan MicroRNA Reverse Transcription Kit (AB). The reactions will be incubated first at 16°C for 30 min and then at 42°C for 30 min. The reactions will be inactivated by incubation at 85°C for 5 min. Each cDNA generated will be amplified by quantitative PCR by using sequence-specific primers from the TaqMan microRNA Assays Human Panel on a Agilent M3005P. The 20µl PCR mix will include 10µl of 2× Universal PCR Master Mix, 2µl of each 10× TaqMan MicroRNA Assay Mix and 1.5µl of reverse transcription (RT) product. The reactions will be incubated at 95°C for 10 min, followed by 40 cycles of 95°C for 15 s and 60°C for 1 min. The threshold cycle (C_T) is defined as the fractional cycle number at which the fluorescence passes the fixed threshold (0.2). All signals with $C_T \geq 37.9$ will be manually set to undetermined. Using the Cancer miRNA qRT-PCR array, while the heat maps were similar across stages, the advanced ovarian cancer patients generally expressed enhanced miRNA expression (Figure 11). This elevated expression within exosomes from Stage III ovarian cancer patients was also observed with the scatter plot (Figure 12).

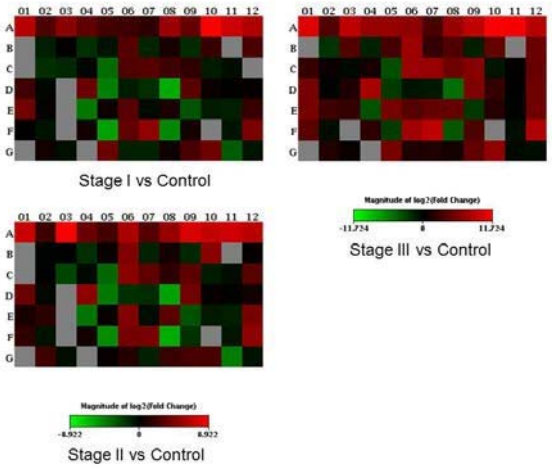

Figure 11: Heat maps of microRNA arrays examining the expression of miRNA in exosomes isolated from ovarian cancer patients at various stages versus controls.

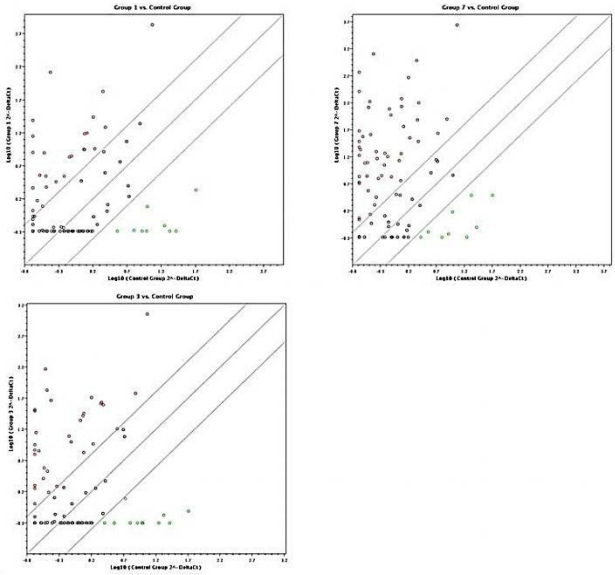

Figure 12: Scatter plot of miRNA expression associated with exosomes from Stage I (Group 1), Stage II (Group 2) or Stage III (Group 3) ovarian cancer

Comparisons between these populations of exosomes derived from cancer patients were not significantly different for most of these miRNAs. The similarity across the stages of ovarian cancer may result from the standardization of starting exosomal small RNA quantities and the normalization of the resulting array data. Despite this standardization and normalization, the profiles obtained with exosomal miRNA from patients with advanced ovarian cancer (Stage III) exhibited some distinct differences (Figure 13). While exosomes derived from all patients with ovarian cancer exhibited similarities, these were distinguished from patients without cancer (both controls and benign disease) and patients with advanced ovarian cancer exhibit a unique signature.

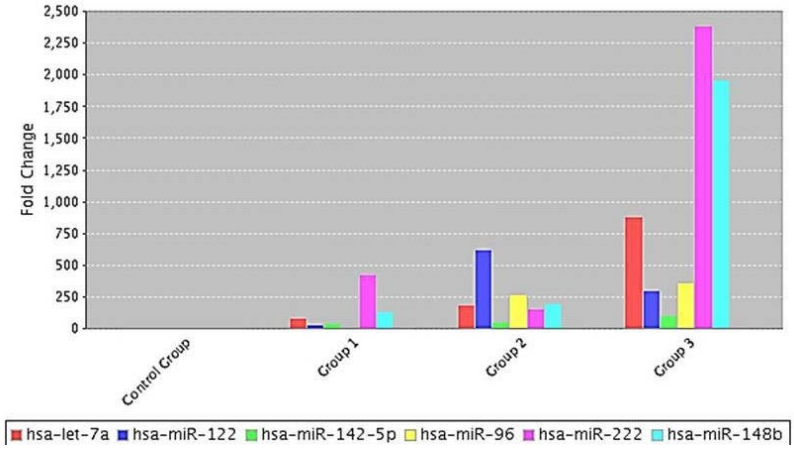

Figure 13: Association of specific miRNAs with stages of ovarian cancer. Control lane represents miRNA isolated from normal controls. Group 1 represents exosomal miRNAs isolated from Stage I, Group 2 corresponds to Stage II and Group 3 to Stage III.

DEMONSTRATION OF lncRNA IN TUMOR-DERIVED EXOSOMES

Long noncoding RNAs (lncRNAs) are master regulators of pluripotency, differentiation, body axis patterning and promoting developmental transitions. LncRNAs represent non-coding RNA that are greater than 200 nucleotides in length. Dysregulation of lncRNA expression has been shown to be associated with a wide range of defects in development and pathologies. Currently lncRNAs have been found to exhibit a wide range of functions ranging from signaling, serving as molecular decoys, guiding ribonulceoprotein complexes to specific chromatin sites and also participating as scaffolds in the formation of complexes.

- **Signaling:** The transcription of certain lncRNAs is very tissue and temporal specific. Their expression can be in response to certain stimuli, such as cellular stress and temperature. Thus, lncRNAs can serve as molecular signals and can act as markers of functionally significant biological events.
- **Decoys:** The molecular decoy type of activity takes place when specific lncRNAs are transcribed and then bind to and titrate away protein factors. Decoy lncRNAs can "sponge" protein factors such as transcription factors and chromatin modifiers. This leads to broad changes in the cell's transcriptome.
- **Guides: l**ncRNAs can be molecular guides by localizing particular ribonucleoprotein complexes to specific chromatin targets. This activity can cause changes in gene expression either in cis (on neighboring genes) or in trans (distantly located genes) that cannot be easily predicted by just the lncRNA sequence itself.
- **Scaffolds:** Assembly of complex protein complexes can be supported by lncRNAs, linking factors to together to form new functions. LncRNAs function as molecular scaffolds regulating histone modifications and influence the epigenetic programs of the transcriptome. Some lncRNAs

possesses different domains that bind distinct protein factors that altogether, may impact transcriptional activation or repression.

While lncRNAs have been identified within cells, we have demonstrated their presence within circulating exosomes. The presence of exosomal lncRNA is demonstrative of the presence of ovarian disease, with specific patterns distinguishing benign and malignant pathologies.

This study analyzed lncRNA within ovarian tumor cell lines and in vitro released exosomes, as well as within exosomes derived from patients with serous papillary adenocarcinoma of the ovary. For ovarian tumor cells, cells were grown in HyClone Serum-free media (SFM). After 3 days, media was removed and centrifuged at 400xg to remove cells and at 10,000xg to remove cell debris. The supernatant was concentrated 10-fold and microvesicles isolated by chromatography using Sepharose 2B. The void volume (vesicle fraction) was treated with Trizol to isolate total RNA. The total RNA fraction was analyzed for specific lncRNAs using the LncRNA profiler qPCR array (Systems Biosciences). Similarly, the tumor cells were directly extracted with Trizol to isolate the RNA fraction and the lncRNAs were analyzed using the LncRNA profiler array. For patient sera, vesicles were isolated using ExoQuick (Systems Biosciences) from 1ml samples of sera obtained from patients with ovarian cancer (n=8) by the manufacturer's instructions. The pelleted vesicles were extracted with Trizol to isolate the RNA fraction and the lncRNAs were analyzed using the LncRNA profiler array. As a control, exosomes were isolated from pooled normal human sera by ExoQuick and total RNA was isolated by Trizol and analyzed in parallel.

Exosomes isolated from the media of cultured tumor cells contain RNA populations. One population identified here was lncRNA. Comparison of lncRNA profiles between tumor cells and their released exosomes reveal selectivity on the lncRNAs appearing in the exosomes. Of the 90 lncRNAs examined, 3 exhibited greater than 10-fold increase in the exosome population. As lncRNA are defined with specific regulatory activity, representative lncRNAs were compared between the cells and their released exosomes. For lncRNAs exhibiting epigenetic silencing, the CT value of ANRIL in cells was 23.80 compared to 26.44 in exosomes. Among lncRNAs exhibiting splicing regulation, the CT value of MALAT-1 in cells was 31.84 compared to 32.85 in exosomes. For lncRNAs regulating apoptosis, the CT value of GAS-5 in cells was 31.72 compared to 29.86 in exosomes. Within lncRNAs expressing translation control, the CT value of BACE1AS in cells was 34.14 compared to 34.86 in exosomes.

LncRNAs were detected within the exosomes isolated from the peripheral circulation of patients. While exosomal lncRNAs can be detected in both cancer patients and normal controls, the lncRNA profiles of cancer patients exhibit profiles distinct from normal (Figure 14). Of the 90 lncRNA analyzed, an increase of greater than 20-fold was observed in 58 lncRNAs in cancer patient-derived exosomes (versus control). In contrast, a decrease of 10-fold or greater was observed in 20 lncRNAs in cancer patients versus controls. Among lncRNAs exhibiting epigenetic silencing, HOTAIR exhibited a 42.85-fold increase in cancer-derived exosomes versus controls. In lncRNAs exhibiting splicing regulation, MALAT-1 was increased 24.7-fold in tumor-derived exosomes compared with controls. For lncRNAs regulating apoptosis, GAS-5 was elevated 30.4-fold in cancer patient-derived exosomes versus controls. Within lncRNAs expressing translation control, BACE1AS was elevated 10,262-fold in patient exosomes versus controls.

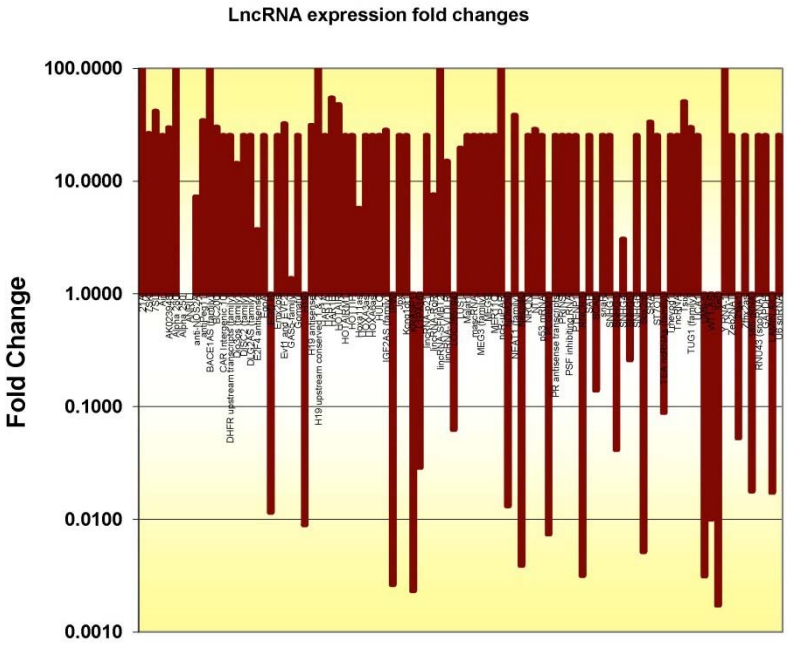

Figure 14: Association of long-noncoding RNA with exosomes from ovarian cancer patients (versus controls).

LncRNAs contribute to genetic regulatory roles, including imprinting, epigenetic regulation, cell cycle control, nuclear and cytoplasmic trafficking, transcription, splicing, cell differentiation and apoptosis. Within tumors, the misexpression of lncRNAs contributes to cancer development and progression. Cancer patients exhibit a significant increased level of circulating vesicles in the range of 50-200nm, which exhibited markers confirming their exosome origin. These exosomes contain lncRNA and their profiles were distinct from non-cancer controls.Some lncRNAs, such as MALAT-1 (metastasis-associated in lung adenocarcinoma transcript) were identified in ovarian cancer and demonstrated to be critical in early stage development. Here we demonstrate the elevation of this lncRNA in exosomes from ovarian cancer patients. The stability of exosomes in the peripheral circulation and the unique profile of lncRNAs suggest their ideal utility as a diagnostic biomarker.

Expanded quantitation and characterization of circulating vesicles in ovarian cancer patients.

A major limitation of DLS and SPA, as well as standard NTA, is that while they can objectively define the vesicle size range, they cannot define the "phenotype" of these vesicles. Using the NanoSight equipped with the 405-nm blue-violet laser and more sensitive camera to detect fluorescent particles, quantum dots attached to antibodies can be used identify specific subsets of vesicles. The instrument was

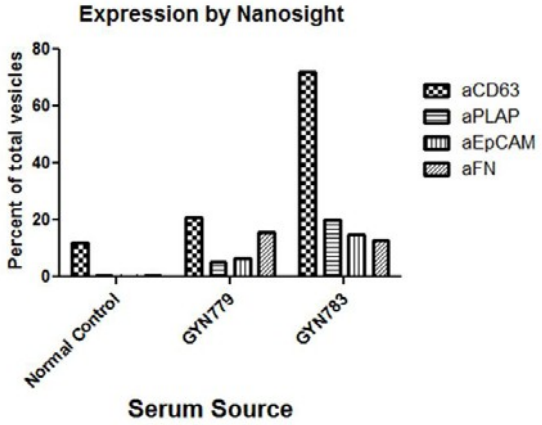

Figure: Expression of specific markers on circulating exosomes defined by Nanosight in fluorescence-mode (compared to total exosomes defined in light scatter mode)

initially calibrated using 100nm and 200nm fluorescent beads, which can be easily discriminated. Antibodies reactive with either CD63 (exosomes marker), EpCAM PLAP, or fetal fibronectin (all previously

demonstrated to be markers of vesicles derived from ovarian tumors) were conjugated with quantum dots. The labeled vesicle samples were analyzed on the NanoSight, first in light scatter mode and then in fluorescence mode. Thus, it is now possible to visualize and quantitate those circulating exosomes derived specifically from the tumor.

Development of asymmetric field flow fractionation from isolation of ovarian tumor exosomes

Asymmetric Field Flow Fractionation (AFFF) is new technology designed for the separation of synthetic nanoparticles. AFFF is a one-phase chromatography technique that generates high-resolution separation within a flow against which a perpendicular force field is applied. The flow and sample are positioned within a channel consisting of two plates that are separated by a spacer foil, with a thickness of 100 to 500 µm. Within the channel, the upper plate is impermeable, while the lower channel plate is constructed of a porous frit material. In the flow channel, a parabolic flow is generated by the laminar flow of the buffer: the stream moves slower closer to the boundary edges than it does at the center of the channel flow. When the perpendicular force field is applied to the flowing, laminar stream, the analytes are driven towards the boundary layer the so-called "accumulation wall" of the channel. Diffusion associated with Brownian motion generates a counteracting motion. The velocity gradient flowing inside the channel separates different sizes of particles. Smaller particles migrate more rapidly through the channel than the larger particles. Since there is no gel media, no shearing forces are applied to the sampel. The entire separation is gentle, rapid, and non-destructive without a stationary phase that may interact, degrade, or alter the sample. We have completed the proof of concept for this approach. We demonstrate the unique presence of the 9-10 minute vesicle peak in ovarian cancer patients. This material is undetectable in all normal.

Separation by AFFF and analysis of vesicular fraction from cancer patients (GYNSR597 and GYNSR472) compared to normal controls by 90° angle static light scattering

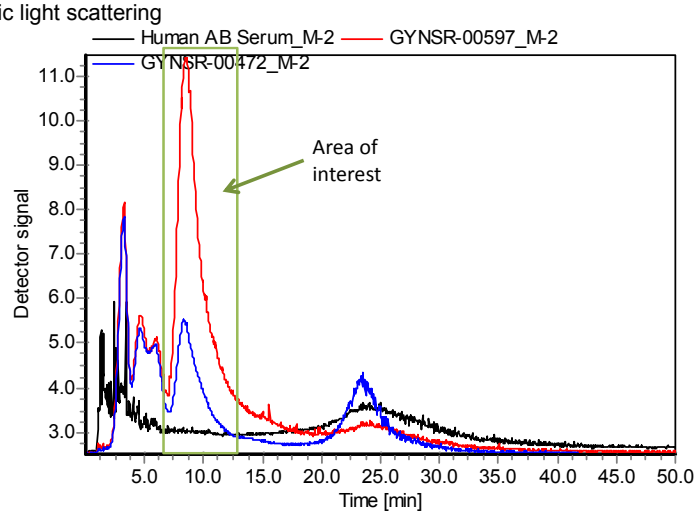

We have developed a non-invasive, high throughput, blood-based exosome platform to address a critical issue - the need to evaluate in real time the state of tumors in individual patients prior to (diagnostic) and in response to therapy. This development addresses the need for biomarkers that serve as predictors or surrogates of therapeutic efficacy. Our hypothesis is that circulating tumor-derived microvesicles and their components can report on the presence, extent and therapeutic responses of ovarian tumors. This proposed commercialization study will provide a comprehensive profile of vesicle populations in blood from ovarian cancer patients by the novel technique of asymmetric field flow fractionation. These analyses will be applied to detect levels and critical characteristics of tumor-derived exosomes in the peripheral circulation to define transcriptome/protein content, which can provide information as to driver mechanisms in individual ovarian tumors. This will correlate specific exosome biomarkers with tumor size and genotype, as well as therapeutic responses and recurrence, survival and clinical status.

This study represents a new paradigm for monitoring ovarian cancer patients. For these patients, exosomal analyses are predicted to facilitate the decision-tree of clinical care. Our goal is to monitor blood-derived exosomal proteomic profiles and transcriptome profiles to identify pathway-response changes in tumors that signal recurrence of ovarian cancer and resistance to treatment. This information will have wide applicability in determining the genotype/phenotype of many types of cancers using easily accessible blood samples and can be combined with other types of biomarker information to give a rapid read-out on response to therapy and mechanisms of resistance to therapy. While soluble individual proteins and nucleic acids are rapidly degraded in the blood, these components when associated with exosomes are stable over time and mirror the

original tumors. A current major challenge and opportunity is the development of methods for rapidly determining the abundance and composition of circulating tumor-specific exosomes from clinical samples. We have developed the high-throughput methodology for isolation of specific tumor-derived exosomes. This approach allows the profiling of tumor-derived exosomes, with unique protein expression levels identifying ovarian cancerfrom host cell exosomes and the utility of exosome profiling to follow cancer treatment efficacy. This approach will quantitate both exosome number and composition as indicators of therapeutic efficacy in clinical trials.

Next generation sequencing analysis of tumor-derived exosomal RNA

The current hypothesis for the stability of circulating RNA is that they are released from cells in membranous vesicles. Recent data confirm that extracellular RNA can exist in four forms: free RNA, Argonaut 2-bound RNA, high-density lipoprotein-bound RNA and vesicle-associated RNA. This review focuses on RNA associated with extracellular vesicles. These extracellular vesicles are generated constitutively by most, but not all, cell types and contain both mRNAs and non-coding RNA. The ability of extracellular vesicles to transfer genetic information may facilitate cancer spread by delivering genetic material and oncogenic proteins. RNA profiles of extracellular vesicles differ from that of cellular RNA, since vesicles contain primarily small RNA, such as mRNA and microRNA, in the absence of ribosomal RNA. The presences of circulating RNAs have been extensively investigated, despite the presence of highly stable RNases, which should degrade any free RNA. The majority of the circulating RNAs have been defined as microRNAs based on the molecular weight. Studies also demonstrated that microRNAs not only have high stability in body fluids, but also survive in the unfavorable physiological conditions such as freeze-thawing, extreme variations in pH and long time at room temperature. Whereas adding detergents, such as Triton X or SDS, to serum or plasma makes microRNAs easily degradation by RNases. The results indicate there are at least two approaches responsible for the stability of extracellular microRNAs: be packaged in membrane-encapsulated vesicle and be protected by RNA-binding proteins.

The stability of extracellular microRNAs has been hypothesized to be due to the formation of the RNA-vesicle. During RISC disassembly in the cytoplasm, some microRNAs are found to be sorted into MVBs, which are commonly considered to form exosomes by fusion with the plasma membrane. Both exosome and microvesicle can easily translocate across the cell membrane, which makes microRNAs enter recipient cells easily and mediate cell-to-cell communication. Our studies have indicated that many of RNAs enriched in the extracellular vesicles may not be abundant, or even detectable, in the originating cell or highly expressed within the cell and low or absent within extracellular vesicles, indicating sorting of specific RNAs into extracellular vesicles. These released microRNAs can be classified in three categories based on the ratio between the amount of microRNA released from the cells and the amount retained in the cell. The first group is selectively released microRNAs, which are characterized by being primarily released from tumor cells with relatively low concentrations remaining in the cell. In contrast, normal cells do not release appreciable quantities of these microRNAs. An additional group of released microRNAs are those released in equal levels as they appear within the cell, termed neutrally released microRNA. These neutrally released microRNAs include miR16 and miR21, where the abundance in extracellular vesicles reflects increased abundance in the tumor cells. The selectivity of release of specific microRNAs differs depending on the cell type. Selectivity appears to be influenced by malignant transformation. Breast and ovarian tumor cells have been demonstrated to release >99% of miR451 and miR1246 produced by the cells. These selectively released microRNAs have been linked to the malignant phenotype. MiR451has been identified as a tumor suppressor, defining proliferation and cell polarity. miR451 has also been shown to induce chemosensitivity. miR1246 induces p53-dependent apoptosis triggered by DNA damage. The changes in the release of cancer-related microRNAs may suggest a role for selective microRNA export in malignant transformation, and it may provide a cancer signature within the exported, circulating microRNA population.

While the mechanism of this selective sorting is unclear, some have postulated this selectivity relates to microRNA/RNA-induced silencing complex (RISC) components. Extracellular vesicles contain components of the microRNA/RISC, such as Argonaut 2, together with several RNA-binding proteins known to regulate RNA traffic between the nucleus and the cytoplasm. It can be therefore hypothesized that, during vesicle biogenesis, these RNA binding proteins regulate the accumulation of selected RNAs within

extracellular vesicles. Studies on the transfer of reporter mRNAs and their translation into proteins, demonstrated both in vitro and in vivo, suggest that the mRNA delivered by extracellular vesicles is functional. Extracellular vesicles derived from other tumors such as colorectal, lung, and prostate cancer cells alter the phenotype of normal cells by transferring specific RNA subsets. In contrast, extracellular vesicles released from the surrounding cells may modify cancer cell gene expression. Extracellular vesicles derived from cancer stem cells were shown to contain pro-angiogenic RNAs able to induce a pre-metastatic niche in the lungs, whereas those derived from differentiated cancer cells were not able to induce this niche and their mRNA and microRNA content differs. Extracellular vesicles from cancer stem cells contained miR29a, miR650, and miR151, all associated with tumor invasion and metastases, along with miR19b, miR29c, and miR151, known to be up-regulated in patients with renal carcinomas.

Extracellular vesicles have been isolated and analyzed from both normal healthy individuals and patients with various physiological conditions. We have previously shown that cancer patients and pregnant women exhibit more extracellular vesicles in their blood compared to their normal, healthy counterparts. In pregnant women, the extracellular vesicles are thought to play a role in the maternal–fetal tolerance occurring during pregnancy, as it has been shown that placenta extracellular vesicles suppress T lymphocytes. Most investigations on small RNAs in exosomes have been limited to microRNA; however, next generation sequencing small RNAs in extracellular vesicles is expanding the populations identified. While intracellular microRNAs have been defined in many biological processes, identification of extracellular vesicle-associated microRNAs represents a non-invasive approach to investigate disease-specific microRNA and may provide a method for disease diagnosis. To detect, analyze, and quantitate the RNA signatures of exosomes derived from biologic fluids, several approaches have been used, including microarrays, quantitative real-time PCR, and next-generation sequencing. The development of high detection sensitivity in next generation sequencing technologies has expanded the identification of the exosomal transcriptome, beyond miRNA. While most studies have focused on exosomal microRNAs, we now recognize the presence of numerous other small RNAs within these circulating exosomes, as well as fragments of larger RNAs. These exosomal small non-coding RNAs are <200 nucleotides in length (generally are 20-30 nt). There are three primary populations of small non-coding RNAs, including siRNAs, miRNAs, and piRNAs. Small non-coding RNAs have been shown to be key regulators in development, apoptosis, stem cell self-renewal, differentiation, and cell integrity maintenance. Piwi-interacting RNAs (piRNAs) are generated from intergenic elements, including transposable elements, through Dicer-independent pathways. These piRNAs function through the Piwi-Argonaute sub-family (AGO3, Aubergine, and Piwi), leading to silencing of transposable elements. A link between piRNAs and cancer has been demonstrated in gastric cancers where two aberrantly expressed piRNAs, piRNA-651 and piRNA-823, were found in gastric tumor tissue versus paired normal tissue.

The transcriptome of circulating EVs provide a real-time monitor of therapeutic response, serving as a companion diagnostic. In 2008, we made the initial demonstration of circulating exosomal RNA. In order to make significant strides in the successful management of ovarian cancer, a paradigm shift to reflecting disease state has to be developed. In this disclosure we report the development of unique exosomal RNA biomarkers for ovarian cancer derived from next generation sequencing. Ovarian masses can be often identified by ultrasound or CT imaging; however, since these approaches generally use morphological criteria and lesion size, they have limited value for detecting microscopic disease or to distinguish benign postoperative changes from tumor recurrence. Our new findings show EV RNA profiles characteristic of ovarian cancer are distinct from those associated with normal or benign ovarian disease.

Extracellular vesicles were isolated from 1ml serum samples of patients with benign ovarian disease and ovarian cancer, as well as a healthy female volunteer and a patient with endometriosis, using the precipitation method (ExoQuick).

SBI Code	Description	NEB Index	Index Sequence
DT-1	LSC4 is the normal female control	1	ATCACG
DT-2	HHE4 is a patient with endometriosis	2	CGATGT
DT-3	GYNSR-00440 is a T3c/N1/M0	3	TTAGGC
DT-4	GYNSR-00719 is a high grade serous carcinoma T3/NX	4	TGACCA
DT-5	GYNSR-00781 is a benign fibrothecoma	5	ACAGTG
DT-6	GYNSR -00784 is a benign serous cyst.	6	GCCAAT

Total RNA was isolated using a phenol-free exosome lysis buffer (SBI). The remaining material was assessed from quality controls by gel electrophoresis and Bioanalyzer.

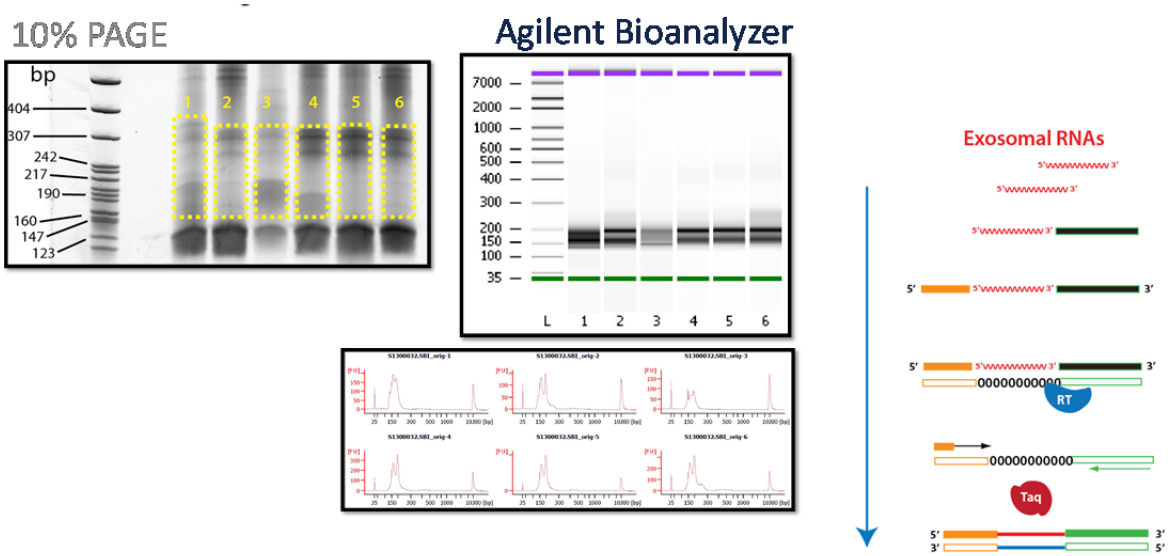

For the resulting exosomal RNA, adapters were initially ligated to the 3' and 5' ends for NGS by standard techniques. This RNA was then subjected to first strand synthesis reverse transcription and amplification with index and PCR. The resulting material was then gel purified. The gel purified material was subjected to NGS. Overall, the exosomal RNA was distributed among antisense transcripts, lincRNAs, LINE, LTR, miRNA, rRNAs, scaRNAs, and tRNAs

We isolated exosomes from 1ml serum samples of patients with benign ovarian disease and ovarian cancer, as well as a healthy female volunteer. Total RNA was isolated using a phenol-free exosome lysis buffer (SBI). The remaining material was assessed from quality controls by gel electrophoresis and Bioanalyzer. For the resulting exosomal RNA, adapters were initially ligated to the 3' and 5' ends for NGS by standard techniques. This RNA was then subjected to first strand synthesis reverse transcription and amplification with index and PCR. The resulting material was then gel purified. The gel purified material was subjected to NGS. Overall, the exosomal RNA was distributed among antisense transcripts, lincRNAs, LINE, LTR, miRNA, rRNAs, scaRNAs, and tRNAs

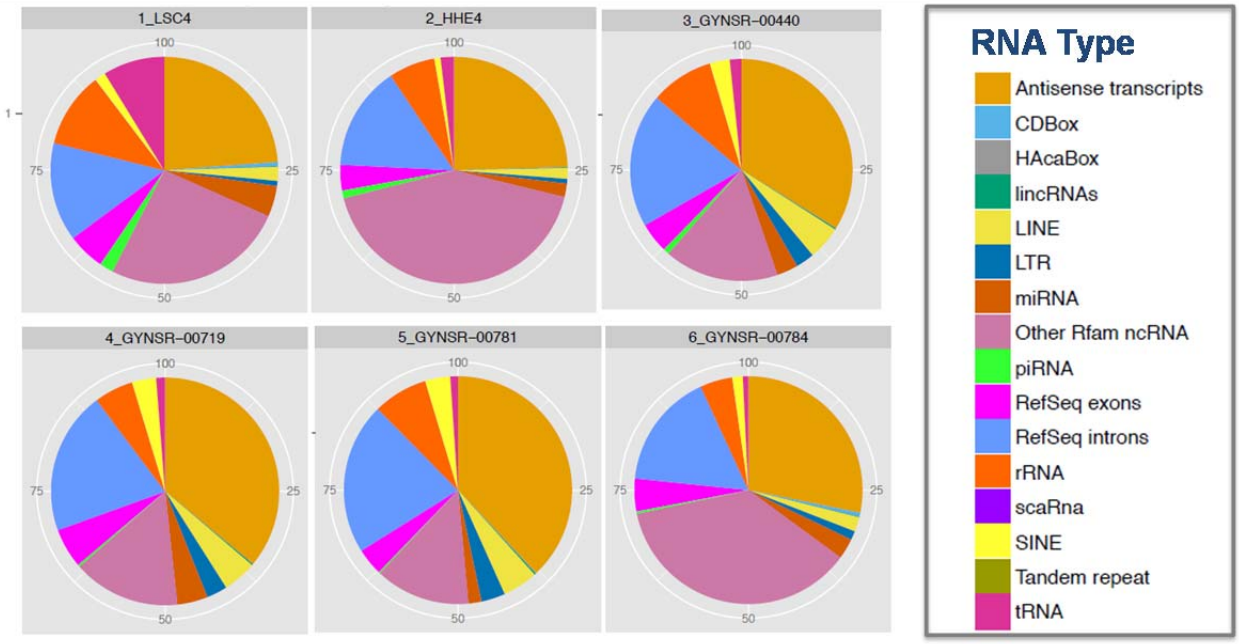

NGS library analysis – Genome mapping

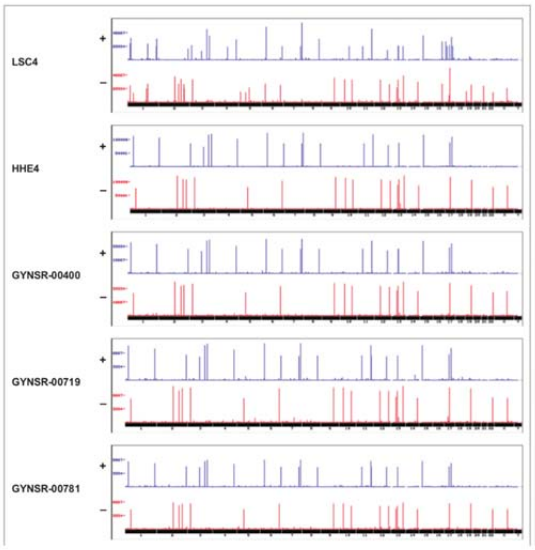

Our analyses of the initial group of ovarian cancer patient samples identified several unique miRNA and tRNA fragments.

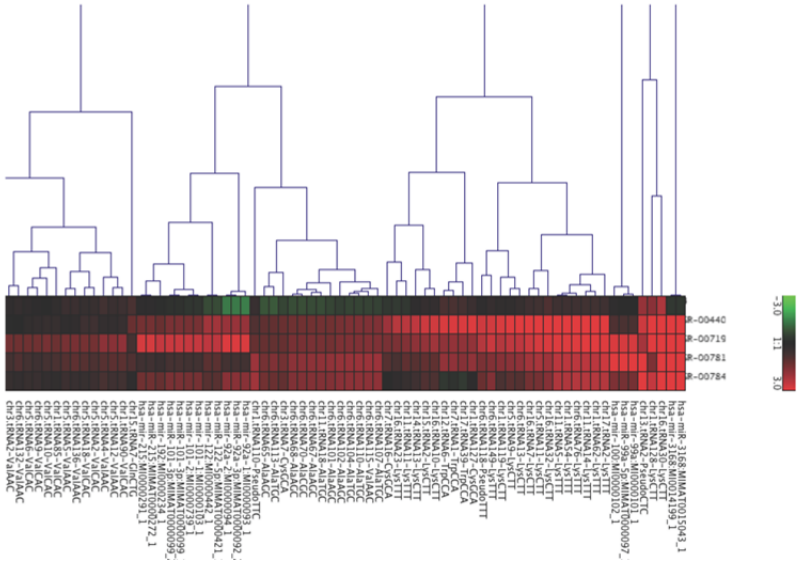

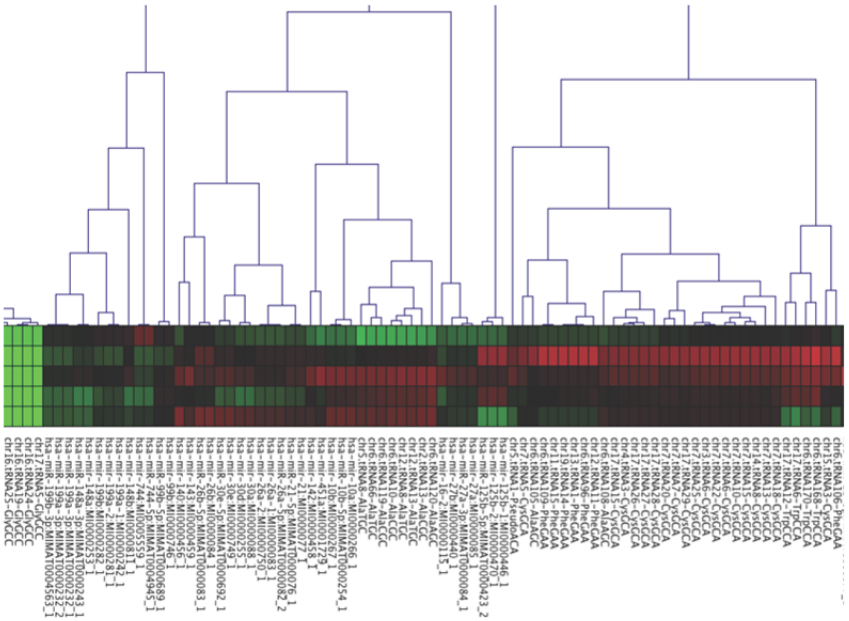

Our analyses of the initial group of ovarian cancer patient samples demonstrated a significant enrichment of the 5’ end of tRNA-Phe-GAA. While this 5’ end fragment is enriched in exosome samples, the 3’ prime fragment is in excess abundance in cellular samples.

miR-3168: Note scales for raw read count are dynamic (numbers on left side of figure). Tracks in red here display total reads on the minus strand, and peak in Sample 3 at 663 counts (S1: 21, S2:15, S3: 663, S4: 127, S5:263, S6: 102). "No data" for plus-strand blue tracks reflects proper strand-specificity of miRNA prediction. No counts seen in any ENCODE data samples for this locus.

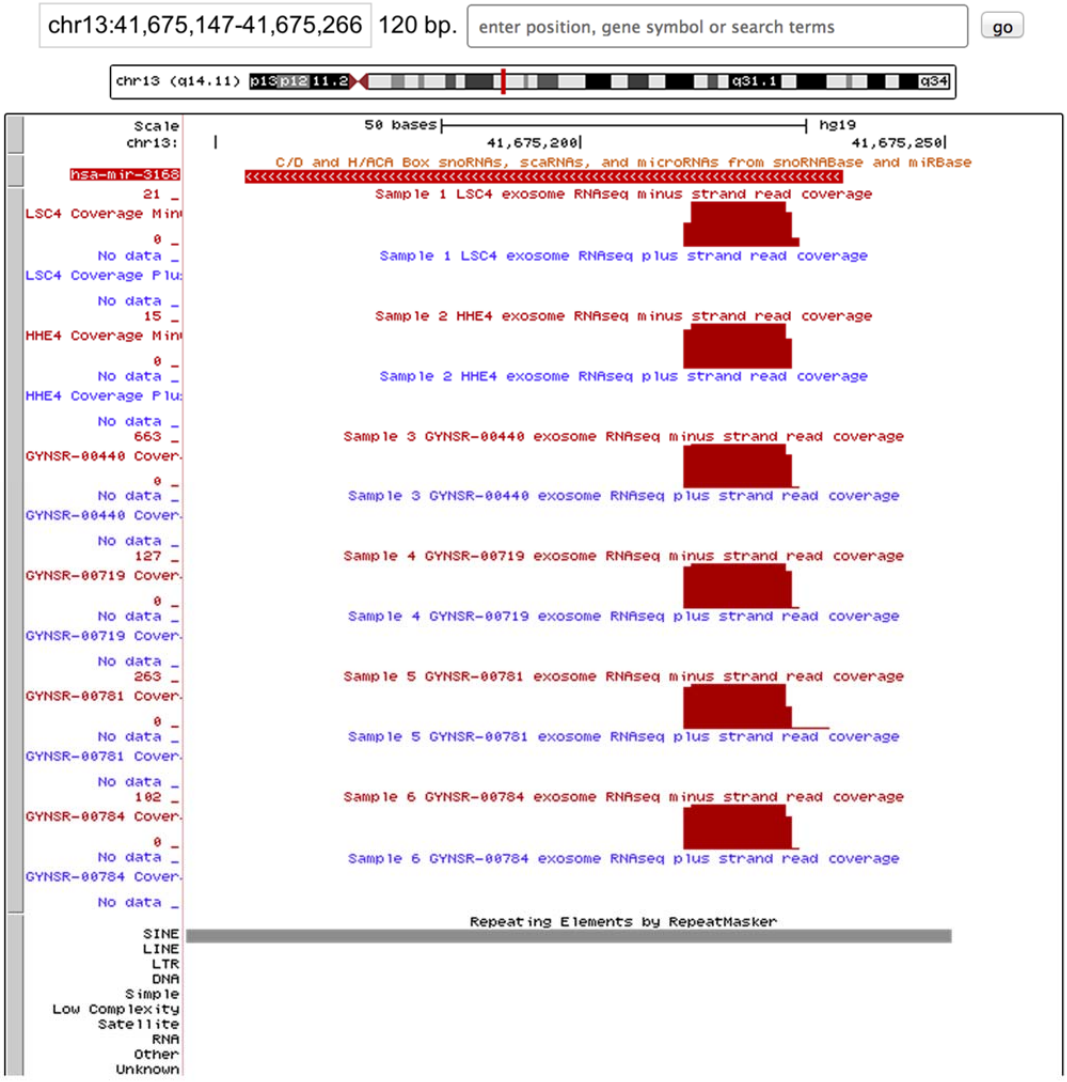

tRNA-Phe-GAA (chr6.trna106): Similar enrichment for 5' end of tRNA as some miRNAs of interest. Note 5' end is enriched in exosome samples, whereas 3' end fragment is in excess abundance in ENCODE cellular samples.

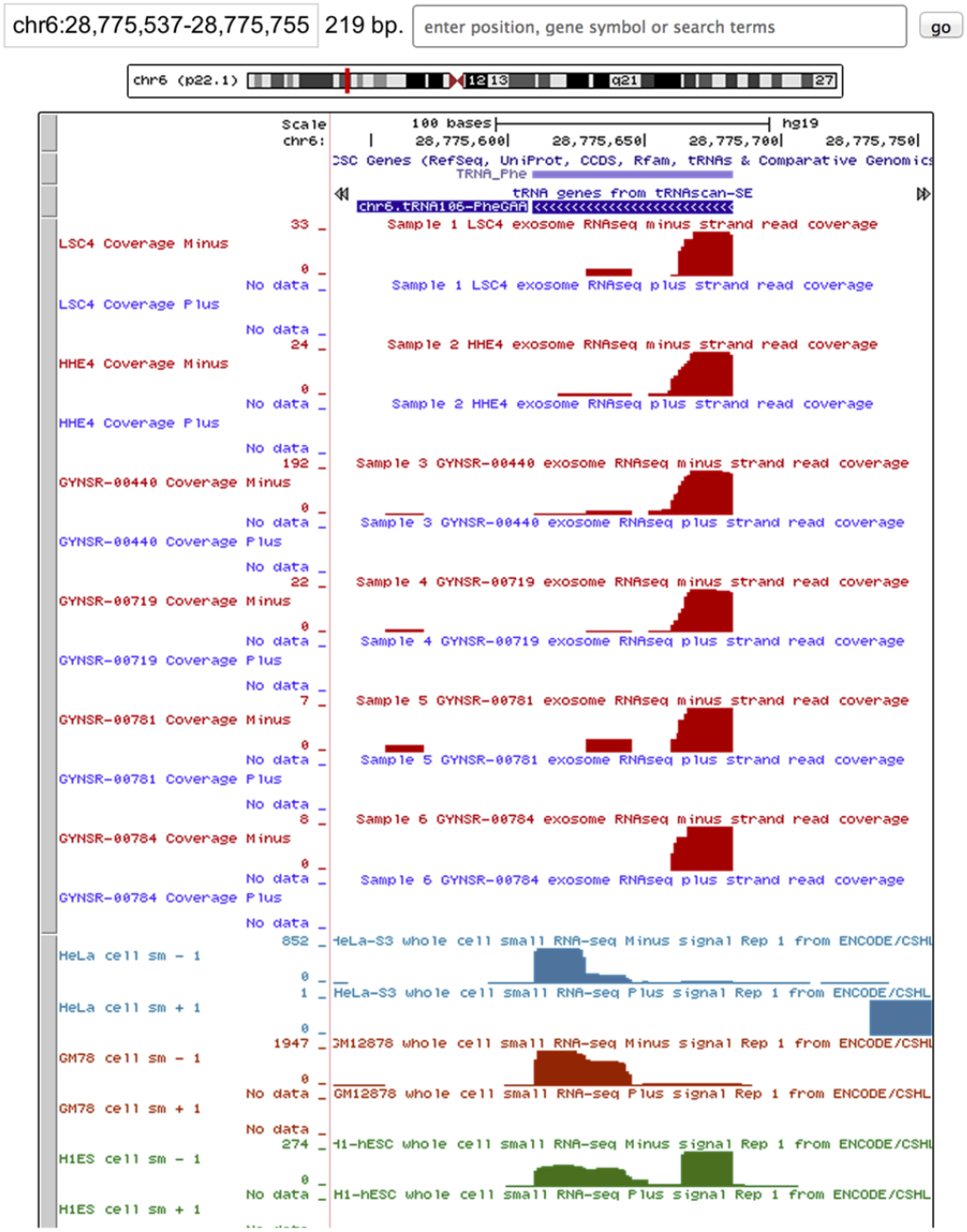

tRNA TrpCCA (chr6.trna170): tRNA enriched in sample 3. Note 3' end enriched in both exosome and ENCODE samples, however pattern of processing is different in exosome samples (note better-defined 5' (right side) end of red peaks in exosome samples, compared to ENCODE samples). Possible signature?

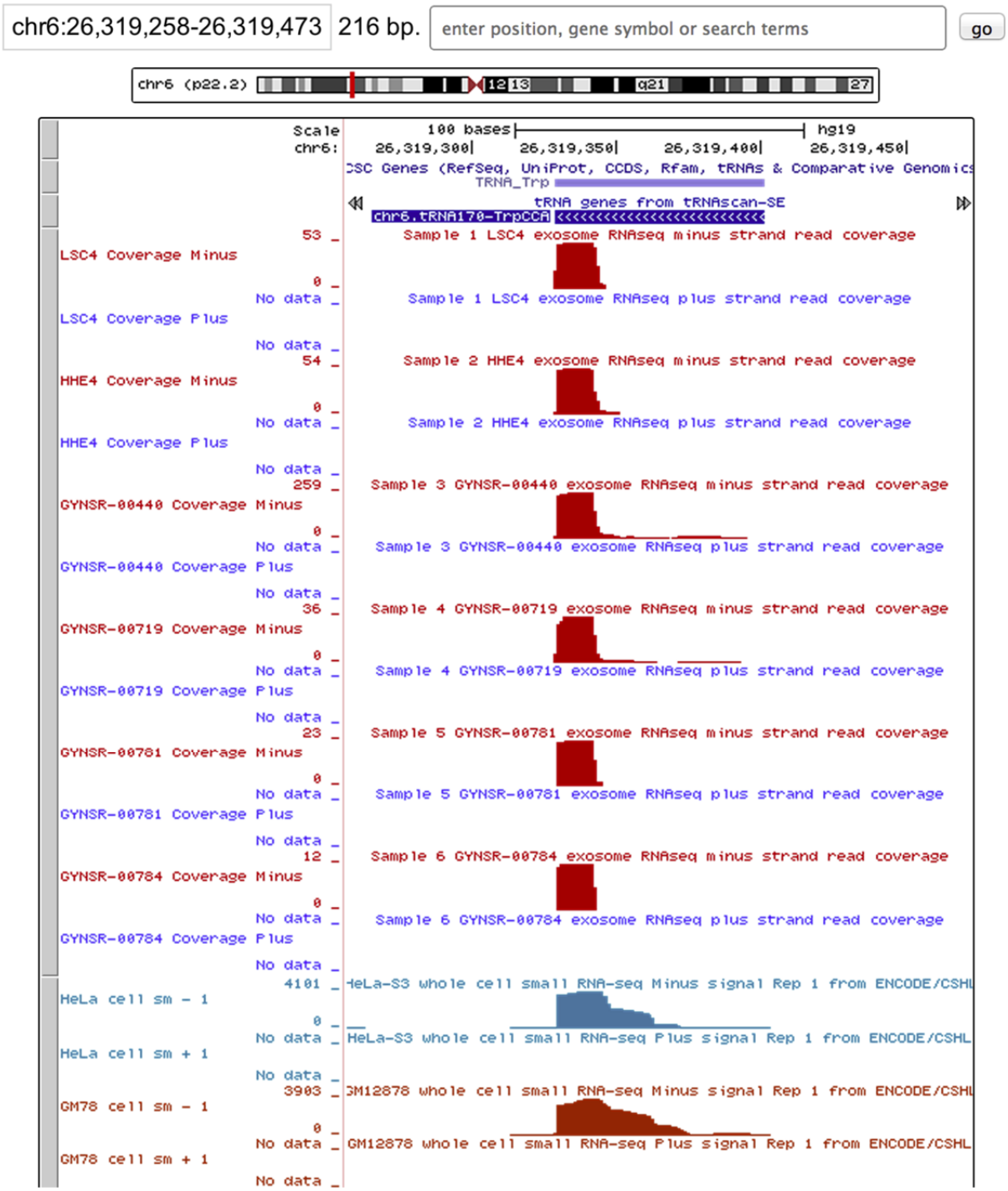

ANALYSES OF EXOSOMES IN NON-SOLID TUMORS

In solid tumors, it has been demonstrated that exosomal signaling plays an essential role in disease progression and therapy resistance. Tumor cells, including AML, release extracellular vesicles that can mediate communication with host components. Our hypothesis is that, in addition to promoting interactions with host immune and stromal components, extracellular vesicles from AML can serve to identify the presence and characteristics of the leukemia. Extracellular vesicles were isolated from 1ml serum samples of patients with AML (n=8) versus normal controls by Sepharose 2B chromatography. The resulting vesicular isolates were characterized by Nanosight for number and size range under light scatter mode and the presence of CD63 under fluorescent mode. The vesicular nature was confirmed by electron microscopy. The presence of exosome and immunological markers was identified by western immunoblotting.

Patients with AML expressed an increased number of circulating extracellular vesicles within their peripheral circulation compared to normal controls ($4.01 \pm 2.11 \times 10^{10}$ for AML versus $1.12 \pm 0.19 \times 10^{10}$, $p = 0.026$). These vesicles exhibited a more uniform diameter than those observed in the control population (mean of 111.6±23.3 nm; mode of 85.3±22.8 nm).

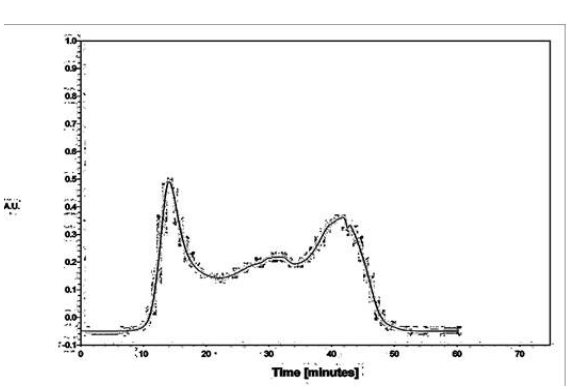

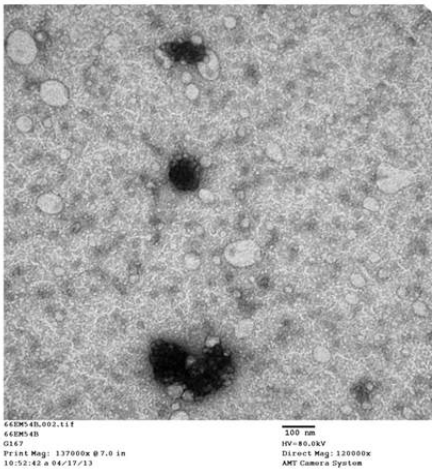

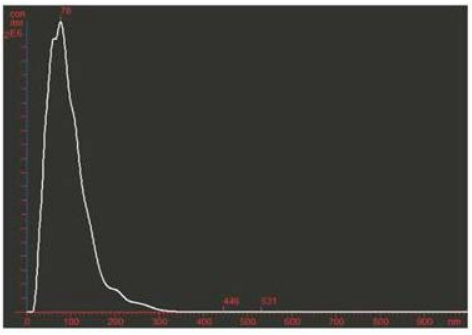

Particle Size / Concentration

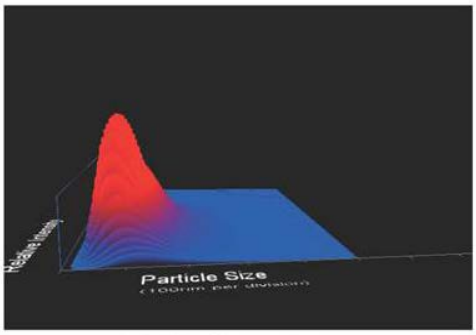

Particle Size / Relative Intensity 3D plot

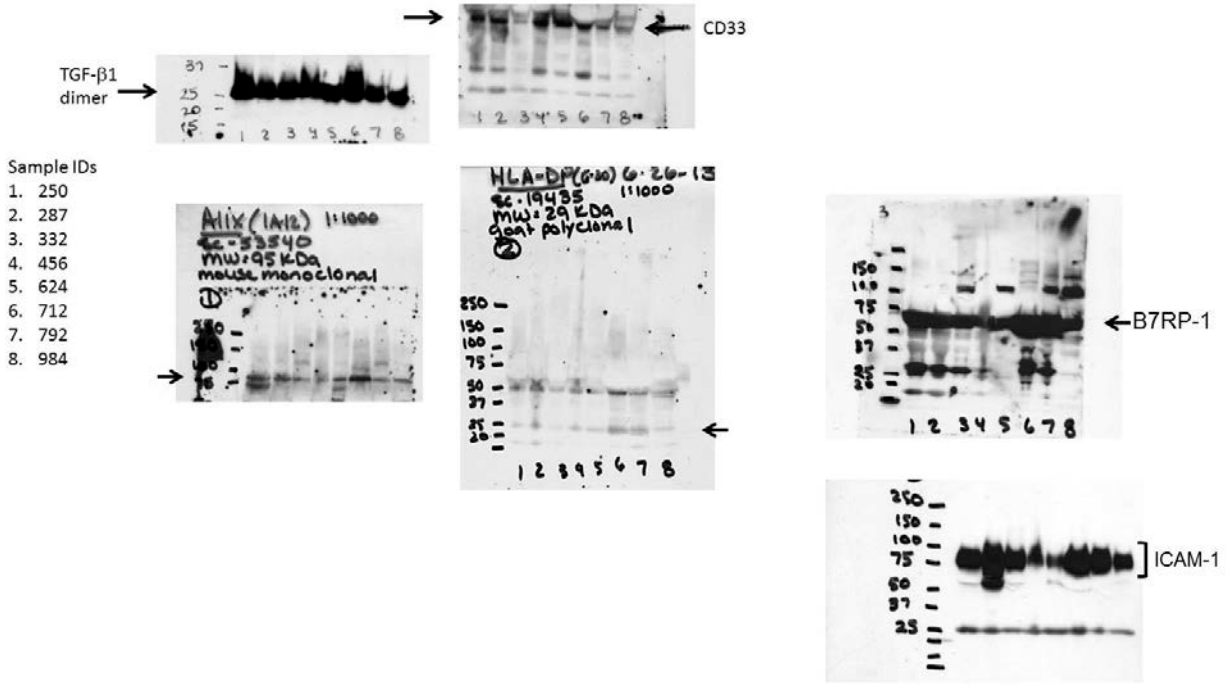

CD63, a marker of exosomes was present over the entire size range. Western immunoblot confirmed the exosome nature of these vesicles based on the expression of CD63 and Alix. In contrast to vesicles derived from normal controls, exosomes from AML patients expressed high levels of the TGF-β, CD33, ICAM-1, B7RP-1 and class-II MHC.

Patients will AML exhibit elevated levels of circulating vesicles that express markers of exosomes. The circulating exosomes also exhibit markers of immunologic status of these patients. Current work is directed at defining whether these vesicles are derived directly from the tumor cells or elicited from normal host components in response to the tumor. In either case, the presence of these exosomes and their associated markers can serve as indicators of tumor presence and disease status.

DEMONSTRATION OF CONSEQUENCES OF TUMOR-DERIVED EXOSOMES OF HOST TARGET CELLS

Many of the miRNAs associated with tumor exosomes have been demonstrated to be associated with regulation of the immune system. For future development of targeted biologic therapeutics, it is essential to define the direct consequences of tumor-derived exosomal miRNA on lymphocyte activation and functions. In an effective immune response, tumor-linked proteins are detected and an anti-tumor response is promoted to eliminate the transformed precursors before they establish malignancy. Effective elimination is characterized by the simultaneous collaboration of innate and adaptive cell-mediated and humoral responses. In the adaptive anti-tumor response, T cells (with cognate TCR) recognize tumor-associated antigens processed/presented on the MHC of antigen-presenting cells (APC), along with subsequent costimulation and cytokine expression for facilitation and maintenance of the response. Elimination of the tumor is accomplished through the activation of cytotoxic T (CTL) cells to induce tumor cell apoptosis, activation of CD4+T cells to promote both cellular and humoral responses through stimulation of APC presentation of antigens to CTL and activation of B cells to produce antigen-specific antibodies that enhance tumor cell

uptake by APCs. The primary anti-tumor response is facilitated by the cellular arm of the adaptive immune system; however, humoral responses to tumour antigens are clearly demonstrated through the production of anti-tumor antibodies. This production of antibodies is presented as elevated IgG in the blood. In ovarian cancer sera, levels of tumor reactive-IgG are elevated, suggesting intact humoral immunity in ovarian cancer patients and an effective humoral anti-tumor response. However, in the midst of this IgG-laden environment, ovarian tumors continue to thrive. A key factor in the progression of transformed cells to malignancy is the tumor microenvironment. The tumor microenvironment consists of a number of cellular participants, including immune cells, which are critical for the suppression of tumor growth. However, the functional activities of these immune cells are often counter-regulated by tumor cell expression and the release of a number of biologic components, which act to promote the growth and metastatic progression of the tumor. One essential biologic component in growth and progression is the tumor derived exosome (TDE). Studies indicate that increased release of exosomes facilitate communication between the tumor's microenvironment and the tumor cell. TDE express tumor-derived antigens; however, they are not molecular duplicates of the plasma membrane of their parental tumor cells; rather, they represent a 'micromap' that displays increased expression of antigens associated with the tumor. TDE are abundantly found in plasma and malignant effusions derived from cancer patients and their presence and expression of tumor-related antigens has been documented to contribute to tumor progression. Progressive effects mediated by TDE have been found to range from regulation of tumor growth to invasion, angiogenesis and metastasis through expression of molecules such as matrix metalloproteinases (MMP-2, MMP-9) and horizontal transfer of growth factor receptors (EGFRvIII). Additionally, TDE have been shown to directly and indirectly modulate the evasion of antitumor responses provided by effector T cells for assisting in progression. Melanoma-derived exosomes have been shown to promote monocyte production of myeloid-derived suppressor cells, which can act to suppress T-cell responses. Ovarian TDE demonstrate induced apoptosis of T cells by enhanced expression of Fas L on the exosomes and CD3zeta suppression on the T cell, while nasopharyngeal TDE have been shown to express increased galectin-9 to induce T cell apoptosis via Tim-3.

Since the activation of B cells and the production of anti-tumor are a hallmark of advanced cancers, this study defined the consequences of tumor-derived exosomes on immature B cells (RA-1) and plasma cells (H929). Tumor exosomes were isolated from patient ascites. The ascites fluids were centrifuged at 400xg for 10 minutes to remove cells and the supernatant was centrifuged at 15,000xg for 20 minutes to remove cell debris. The resulting supernatant was concentrated by ultrafiltration using an Amicon stirred cell with a molecular weight cut-off membrane of 500,000 Daltons (Millipore). This concentrated material was then chromatographically separated using a Sepharose 2B column (2.5x30cm). The void volume fractions were pooled and centrifuged at 100,000 x g for 1 hour at 4°C. The pellet was resuspended in PBS and the protein concentration determined using the DC protein assay. To exclude the possibility of endotoxin contamination in the exosome preparations for ascites-derived vesicles, a LAL assay (Genscript, Piscataway, NJ) was performed to quantify any endotoxin in the vesicle preparations.

To define the effects of tumor-derived exosomes on B cell chemokine and cytokine profiles, their productions by RA-1 and H929 cells were quantified with duplicate arrays, each having duplicate spots for each cytokine using Proteome profiler™ Human Cytokine Antibody Array Panel A Arrays (R&D Systems, Minneapolis, MN) according to the manufacturer's instructions. The B cell lines were incubated with 100µg/ml tumor-derived exosomes or untreated for 20 hours. The cytokine array membranes were incubated with 1ml of conditioned media from each sample, diluted 1:3 and 15µl of Cytokine Array Panel A detection antibody at 4°C overnight. The membranes were then washed three times with 20 ml of 1× wash buffer and incubated with horseradish peroxidase-conjugated streptavidin (1:2000-dilution). After 30 minutes, the membranes were washed thoroughly and exposed to a chemiluminescent peroxidase substrate for 5 min in the dark before imaging. Membranes were exposed to x-ray film (Research Products International, Mt Prospect, IL). As per the manufacturer's package insert, the cytokine array data on developed X-ray film was quantitated by scanning the film on a transmission-mode scanner and analyzing the array image file using image analysis software, Un-Scan-it gel digitizing software version 6.1 (Silk Scientific Corporation, Orem, UT). Positive controls at three spots were used to identify membrane orientation and to normalize the results from different membranes. For each spot, the specific pixel level was determined by subtracting the background pixels from the total raw pixel levels. To quantify relative change in cytokine levels between

samples, the average background-subtracted mean spot pixel densities of the pair of duplicate spots representing each cytokine was determined for each condition. To facilitate further analyses, all spots in the arrays were quantified and their specific intensity values were obtained by subtracting the background intensity. Only differences in cytokine levels that were ≥ 2-fold compared to controls were considered significant.

Following incubation of the B cell lines with tumor-derived exosomes, total RNA from the exosome-treated and untreated B cells were extracted by Trizol. The profiles of 88 specific RNAs, associated with lymphocyte activation and function were analyzed in each population using RT-PCR arrays (Qiagen).

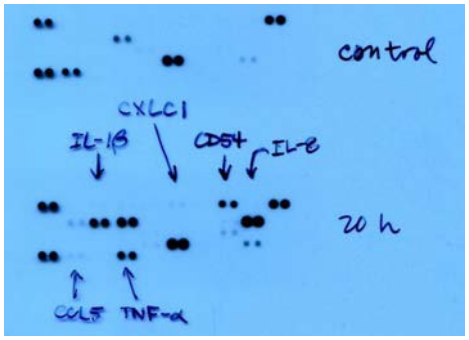

Figure: Representation cytokine array showing the production of specific cytokines and chemokines in untreated B cells compared to B cells exposed to 100ug tumor exosomes for 20 hours.

Based on the cytokine/chemokine arrays, exposure of B cells to tumor-derived exosomes induced those cytokines associated with B cell activation, but not T cell activation. Additional analyses of mRNA associated with exosome-treated B cells (Attachment 4) revealed that:

In RA-1 cells exposed to tumor exosomes for 5h and 16 h -
- exosome exposure increased expression of IL-10
- exosome exposure enhancedexpression of IL-6
- in the presence of CD40L and IL-4, exosomes exhibited an additional enhancement in IL-6 expression
- at 5h, the presence of tumor exosomes elevated expression of AID.

In H929 cells exposed to tumor exosomes for 5h and 16h -
- exosomes increased expression of IL-10, with an additional increase observed at 16h
- while the addition of CD40L alone increased expression of IL-10, the further addition of exosomes induced a greater enhancement of IL-10 expression
- exosomes at 5h elevated expression of IL-4

Under these conditions, genes associated with T cell activation were either suppressed or unchanged.

CONCLUSIONS

Cell-derived vesicles and exosomes are potential markers of human disease. This could include the identification of elevated circulating exosomes and the presence of specific exosome "cargo." However, their use in diagnostic tests requires an objective and high throughput method of defining their size, concentration, and phenotype in biological fluids. Current methodologies cannot achieve this definition and characterization.

Recognizing this critical issue, during the past 12-month funding period, we demonstrated the feasibility of using nanoparticle tracking analysis (NTA). Although NTA is relatively new and still developing, this technology is well established in other fields, particularly for the measurement of engineered nanoparticles, carbon nanotubes, inks and pigments, and viral particles. The ultimate application of exosome-based diagnostic markers is the ability to identify the presence of circulating cell-derived vesicles and their concentration and size distribution in clinical specimens. We determined the presence and distribution of circulating vesicles in unfractionated sera from

ovarian cancer patients, patients with benign disease and female controls (Figure 1). Using the NanoSight LM10, ovarian cancer patients were shown to exhibit ~4-fold increase in the level of total circulating vesicles. The size distribution of these unfractionated vesicles from cancer patients ranged from approximately 50 to 300nm in diameter. Patients with benign disease and controls exhibited a similar size range; however, they possessed a greater percentage of vesicles within the 200-300nm range (versus cancer).

We demonstrated that fractionation of bio-fluids on Sepharose 2B results in two primary peaks of material (Figure 2A): a void volume and a retained peak. We analyzed the individual fractions of the void volume (fractions 15, 16, and 17) using the Nanosight LM10 and NTA software (Figure 2B). NTA demonstrated a very narrow size range of vesicles, with fraction 15 contained vesicles ranging from 50-200nm with a primary peak at 94nm (mode = 94nm, mean = 108, SD = 30nm). Fraction 16 exhibited vesicles also ranging from 50-200nm, but the primary peak appeared at 89nm (mode = 89nm, mean = 95nm, SD = 32nm). Fraction 17 consisted on vesicles ranging from 50-200nm with two principal vesicle peaks at 84nm and 108nm (mode =84, mean = 109, SD =30). Our results demonstrated that the majority of the vesicles within the void volume fractions fall within the 50-100 size range described for exosomes. To define the identity of these vesicles, the current "gold standard" is Western immunoblotting for specific marker proteins. Western immunoblotting of the individual fractions for specific markers claimed to be associated with either exosomes (tetraspanin CD63) or microvesicles (CD154, as known as CD40 ligand). Western immunoblot analysis demonstrated the combined expressions of CD63 and CD154 within the void volume fractions that demonstrate an exosome size distribution. The mutant EGFRvIII, generally considered to be associated with the plasma membrane of cancer cells also appears to be associated with these void volume vesicles, demonstrating the tumor origin of this material. While these vesicles are within the size range of exosomes, they exhibit markers previously defined both as markers for exosomes and microvesicles. Thus, this distinction may not be relevant for clinical specimens.

The "gold standard" for defining the size and characteristics of exosomes is electron microscopy to demonstrate the presence of cup-shaped vesicles, ranging from 50-100nm. This size range was initially defined using exosomes derived from normal lymphocytes. One issue is that size can be modified by sample preparation for EM and the size distribution can be skewed by the image area selected for evaluation (subjective). Since EM studies use pelleted vesicles, image fields where individual vesicles can be visualized may be a limiting factor in this selection. In general, light scattering methodologies report a larger size range than EM and evaluate objectively the total vesicle populations. This study compared these methodologies using chromatographically isolation vesicles. NTA, SPA and DLS were compared with electron microscopic analysis of vesicles: For electron microscopy, the size distribution of vesicles was determined by measuring their diameters directly from electron micrographs of ultracentrifuge pellets. NTA gave a vesicle size distribution from 50 to 175 nm with a mean = 100nm, mode = 87 and SD = 28. Analysis of the same vesicle preparation by DLS indicated a mean diameter of 125.3 ± 1.9nm, while the submicron particle analysis indicated a range of 80 to 120nm. Although the area of the electron microscopy image selected contains vesicles between 50-100nm, While in general EM has been shown to lead to undersizing, vesicles larger than 100nm are clearly visible in multiple fields and the real size distribution of the entire vesicle population is not assessable and EM is not quantitative. DLS and SPA, while providing an objective size distribution of the entire vesicle population, do not define the concentration of the vesicles.

A significant limitation of DLS and SPA is that while they can objectively define the vesicle size range, they cannot define the "phenotype" of these vesicles. Using the NanoSight LM10 equipped with the 405-nm blue-violet laser and more sensitive camera to detect fluorescent particles, quantum dots labeled antibodies reactive with either CD63 (exosomes marker) or EpCAM (marker of vesicles derived from epithelial tumors) labeled vesicles with peaks in the region of 100 nm and 180 nm whether measured in light scatter or fluorescence mode. Vesicles both larger and smaller than 100nm exhibit CD63 demonstrating that the published definition of exosomes as ranging only from 50-100nm may not be accurate.

A criticism of light scattering, Brownian motion based technologies is that these methods do not

adequately differentiate between synthetic nanoparticles, large protein aggregates and biologic vesicles. In our size exclusion approach, the void volume fractions contain materials greater than 50 million Daltons, which would be expected to distinguish vesicles from large protein aggregates, including large immune complexes. However, in order to validate that we are differentiating vesicles from large protein complexes, the chromatographically isolated vesicles were initially analyzed by SPA and NTA, followed by a re-analysis after a 5 minute treatment with a non-ionic detergent. Using SPA on the Coulter Model N4 Plus particle size analyzer, the values for vesicle size was observed to range from 80-100nm. Following treatment with 1% Tween 20 for 5 minutes at room temperature, the reanalysis shown that the average size of the particles shifted ~10nm (range 5-20 nm). Using a similar approach with NTA, the same sample treated with 0.5% Triton X100 for 5 minutes at room temperature exhibited a 10-fold reduction.

Vesicle analyses based on light scattering and Brownian motion analyses allow quantitation of mean vesicle size and size distribution. NTA has the additional advantage of defining concentration. The disadvantage of SPA and DLS is that they are unable to determine the phenotype of the vesicles. Since biological fluids and clinical specimens comprise mixtures of vesicles derived from many different cell types, it is essential to be able to determine the cell of origin and to understand their biological function, the molecules that they express on their surface.

An addition critical issue is the separation of tumor-derived exosomes from exosomes released by normal cells presence within the peripheral circulation. To define diagnostic tumor markers, it is essential to identify those actually derived from the tumor. While cell-derived vesicles can be released from many cell types, their accumulation within the peripheral circulation appears to be elevated 3-4-fold in cancer patients. However, since only a fraction of these are produced by the tumor, differentiating the tumor-derived from normal cell-derived exosomes has been problematic. The "background of normal cell-derived exosomes results in significant "noise" in studies failing to separate the tumor-derived exosomes. We have now isolated exosomes from the peripheral circulation of patients with ovarian cancer or from non-tumor-bearing controls by size exclusion chromatography. Further isolation of tumor-specific exosomes by our proprietary method revealed a subpopulation of vesicles within the peripheral circulation with the mean diameter at 72nm. The number of vesicular particles was also determined by the Nanosight analysis, demonstrating the presence of 2.46×10^{10} vesicles/ml (Figure 8). As a proof of concept that the tumor-derived exosome fraction was being isolated, we demonstrated the enrichment of a tumor-specific population was confirmed by the enhanced expression of the tumor marker, EGFRvIII (Figure 9). Thus, analyses of the "cargo" of this enriched tumor derived exosome fraction will allow us to specifically define markers of tumor status and not markers of the patient's normal cell response to the tumor. This is critical as the host response is likely to be non-specific (such as a pro-inflammatory immune response) and could result in significant false positive results.

A third critical finding is the selectivity of the exosomal "cargo." To date, analyses of exosomes and their components have been based on markers demonstrated within the tumor cell and in particular elements apparently up-regulated in the original tumor cells. It has been postulated that components within exosomes are a direct extension of the originating cell. However, our data demonstrate that the miRNAs appearing within the exosomes are highly selective (Figure 10). Of 10 miRNAs on the Cancer miRNA qRT-PCR array previously demonstrated top be elevated in ovarian tumor cells, 8 exhibited significant elevations (greater than 2-fold. 7 miRNAs have been reported to be down-regulated in ovarian tumor cells. Of these, 7 miRNAs only 1 expressed a down-regulation of more than 2-fold (miR-203). Six of these miRNAs were up-regulated by more than 2-fold within exosomes. These results suggest that certain specific miRNAs are "packaged" within exosomes, with little of these miRNAs remaining within the originating cells. In contract, miRNAs up-regulated within the tumor cells appear to be mirrored by their expression within the exosomes. Thus, we now recognize that some crucial exosomal miRNA markers may not be detectable within the tumor cells.

A fourth finding of the past 12-month funding period was the discovery of long-non-coding RNA. In addition to proteins, lipids and miRNAs, our current work has demonstrated the present of long noncoding RNAs within exosomes. LncRNAs contribute to genetic regulatory roles, including imprinting, epigenetic regulation, cell cycle control, nuclear and cytoplasmic trafficking, transcription, splicing, cell differentiation and apoptosis. In cancer, the misexpression of lncRNAs contributes to cancer

development and progression. Cancer patients exhibit a significant increased level of circulating vesicles in the range of 50-200nm, which exhibited markers confirming their exosome origin. These exosomes contain lncRNA and their profiles were distinct from non-cancer controls. Some lncRNAs, such as MALAT-1 (metastasis-associated in lung adenocarcinoma transcript) were identified in ovarian cancer and demonstrated to be critical in early stage development. Here we demonstrate the elevation of this lncRNA in exosomes from ovarian cancer patients (Figure 14). The stability of exosomes in the peripheral circulation and the unique profile of lncRNAs suggest their ideal utility as a diagnostic biomarker.

PUBLICATIONS

1. Xiang X, Liu Y, Zhuang X, Zhang S, Michalek S, Taylor DD, Grizzle W, Zhang HG TLR2 mediated expansion of MDSCs is dependent on the source of tumor exosomes. *American Journal of Pathology*, **177**: 1606-1610, 2010.
2. Atay S., Gercel-Taylor C., Kesimer M., Taylor, D.D. Morphologic and proteomic characterization of exosomes released by cultured extravillous trophoblast cells. Experimental Cell Research, **317**: 1192-1202, 2011.
3. Taylor, D.D., Zacharias, W., and Gercel-Taylor, C. Exosome isolation for proteomic analyses and RNA profiling. In: Methods in Molecular Biology (RJ Simpson, ed), **728**: 235-246, 2011.
4. Taylor, D.D., Gerçel-Taylor, C.: Exosomes/Microvesicles: Mediators of cancer-associated immunosuppressive microenvironments. Seminars in Immunopathology, 33:441-54, 2011.
5. Roberson, C., Atay, S., Gercel-Taylor, C., Taylor, D.D.: Tumor-derived exosomes as mediators of disease and potential diagnostic biomarkers. Cancer Biomarkers: Biomarkers in Ovarian cancer, (A. Lokshin and W. Tainsky eds.), 8:281-291, 2011.
6. Gercel-Taylor C, Taylor DD, Rai SN. Proteomic identification of serum peptides predicting subsequent spontaneous preterm births. *American Journal of Obstetrics & Gynecologiy,*206:e3, 2012.
7. Xiao D, Ohlendorf J, Chen Y, Taylor DD, Rai SN, Waigel S, Zacharias W, Hao H, McMasters KM. Identify mRNA and microRNA and protein profiles of melanoma exosomes. *PLoS One*, **7**:e46874, 2012.
8. Simpson R.J., Kalra H., Ji H., Altevogt P., Askenase P., Breakefield X., Buzas E., Camussi G., Clayton A., Gabrielsson S., Gho Y.S., Harsha H.C., Hill A.F., Jenster G., Kiang L.S., Llorente A., Mincheva-Nilsson L., Nazarenko I., Nieuwland R., Pandey A., Pluchino S., Prasad T.S., Rajendran L., Raposo G., Record M., Reid G.E., Sanchez-Madrid F., Stoorvogel W., Taylor D., Thery C., Vidal M., Zoeller M., Mathivanan S. Vesiclepedia: A compendium for extracellular vesicles that enables continuous annotation. *PLoS One* **10**:e1001450, 2012.
9. Atay, S., Roberson, C., Gercel-Taylor, C., Taylor, D.D. Ovarian cancer patient-derived exosomal fibronectin induces pro-inflammatory IL-1β production by macrophages. *Exosomes and Microvesicles,* 1, 1, 2013.
10. Taylor, D.D., Gercel-Taylor, C. The origin, function, and diagnostic potential of RNA within extracellular vesicles present in human biological fluids. *Front. Genet*. **4**:142, 2013.

REFERENCES

1. Jemal A, Murray T, Ward E, Samuels A, Tiwari RC, Ghafoor A, Feuer EJ, Thun MJ. Cancer statistics, 2005. CA: A cancer J for Clinicians, 55:10-30, 2005.
2. Division of Cancer Prevention and Control, National Center for Chronic Disease Prevention and Health Promotion, 2006.
3. Berek JS, Schultes BC, Nicodemus CF. Biologic and immunologic therapies for ovarian cancer. J Clin Oncol 2003; 21(suppl 10): 168-174.
4. Memarzadeh S, Berek JS: Advances in the management of epithelial ovarian cancer. J Reprod Medicine 46:621-629, 2001.
5. Hoskins WJ: Prospective on ovarian cancer: Why prevent? J Cell Biochem 23 (suppl):189-199, 1995
6. Taylor DD and Gercel-Taylor C: Tumor reactive immunoglobulins. Oncology Reports, 1998.
7. Bast RC Jr, Klug TL, St John E. A radioimmunoassay using a monoclonal antibody to monitor the course of epithelial ovarian cancer. New Engl J Med, 309:883-887, 1983.
8. Juretzka MM, Barakat RR, Chi DS, Iasonos A, Dupont J, Abu-Rustum NR, Poynor EA, Aghajanian C, Spriggs D, Hensley ML, Sabbatini P. CA125 as a predictor of progression-free survival and overall survival in ovarian cancer patients with surgically defined disease status prior to the initiation of intraperitoneal consolidation therapy. Gynecol Oncol, 104:176-180, 2007.
9. Menon U, Jacobs IJ. Recent developments in ovarian cancer screening. Curr Opin Obstet Gynecol, 12:39-42, 2000.
10. Petricoin EF, Ardekani AM, Hitt BA, Levine PJ, Fusaro VA, Steinberg SM. Use of proteomic patterns in serum to identify ovarian cancer. Lancet, 359:572-577, 2002.
11. Zhang H, Kong B, Qu X, Jia L, Deng B, Yang Q. Biomarker discovery for ovarian cancer using SELDI-TOF-MS. Gynecol Oncol, 102:61-66, 2006.
12. Jacobs IJ, Menon U. Progress and challenges in screening for early detection of ovarian cancer. Mol Cell Proteomics, 3:355–366, 2004.
13. Taylor DD, Homesley HD, Doellgast GJ (1980) Binding of specific peroxidase-labeled antibody to placental-type alkaline phosphatase on tumour-derived membrane fragments. Cancer Res 40: 4064–4069
14. The´ry C, Regnault A, Garin J, Wolfers J, Zitvogel L, Ricciardi-Castagnoli P, Raposo G, Amigorena S (1999) Molecular characterization of dendritic cell-derived exosomes. Selective accumulation of the heat shock protein hsc73. J Cell Biol 147: 599–610
15. The´ry C, Zitvogel L, Amigorena S (2002) Exosomes: composition, biogenesis, and function. Nat Rev Immunol 2: 569–579.
16. Taylor DD, Lyons KS, Gerc¸el-Taylor C (2002) Shed membrane fragment associated markers for endometrial and ovarian cancers. Gynecol Oncol 84: 443–448
17. Monleon I., M. J. Martinez-Lorenzo, L. Monteagudo, P. Lasierra, M. Taules, M. Iturralde, A. Pineiro, M. A. Alava, J. Naval, and A. Anel. 2001. Differential secretion of Fas ligand or APO2 ligand/TNF-related apoptosis-inducing ligand-carrying microvesicles during activation-induced death of human T cells. *J. Immunol*. 167:6736-6744.
18. Raposo, G., D. Tenza, S. Mecheri, R. Peronet, C. Bonnerot, and C. Desaymard. 1997. Accumulation of major histocompatibility complex class II molecules in mast cell secretory granules and their release upon degranulation. *Mol. Biol. Cell*. 8: 2631-2645.
19. Heijnen, H. F. G., A. E. Schiel, R. Fijnheer, H. J. Geuze, and J. J. Sixma. 1999. Activated platelets release two types of membrane vesicles: Microvesicles by surface shedding and exosomes derived from exocytosis of multivesicular bodies and alpha granules. *Blood* 94, 3791-3799.
20. Taylor DD, Black PH (1986) Shedding of plasma membrane fragments: Neoplastic and developmental importance. In: Developmental Biology (vol. 3), Steinberg MS (ed) pp 33-57. Plenum Press: New York.
21. Taylor DD, Black PH (1987) Neoplastic and developmental importance of plasma membrane vesicles. Amer Zool 26: 411–415

22. Taylor, D.D., Gerçel-Taylor, C., and Weese, J.L. Expression and shedding of mdr-1 antigen by variants of the murine B16 melanoma. Surgical Forum, 40:406-408, 1989.
23. Bazzett, L.B., Magnus, M., Taylor, D.D., Gercel-Taylor, C. Urinary matrix metalloproteinases as a potential screening test for gynecologic malignancies. Gynecologic Oncology, 90:435-442, 2003.
24. Taylor, D.D., Gerçel-Taylor, C., and Gall, S.A. Expression and shedding of CD44 isoforms by gynecologic cancer patients. Journal of the Society for Gynecologic Investigations, 3:289-294, 1996.
25. Taylor, D.D., Lyons, K.S., and Gercel-Taylor, C. Shed membrane fragment-associated markers for endometrial and ovarian cancers. Gynecologic Oncology, 84:443-448, 2002.
26. Mor G, Gutierrez LS, Eliza M, Kahyaoglu F, Arici A. Fas-Fas ligand system-induced apoptosis in human placenta and gestational trophoblastic disease. Am J Reprod Immunol, 40:89-94, 1998.
27. Taylor DD, Sullivan SA, Eblen AC, Gercel-Taylor C. Modulation of T-cell CD3-zeta chain expression during normal pregnancy. J Reprod Immunol, 54:15-31, 2002.
28. Taylor DD, Gercel-Taylor C. Tumor-derived exosomes as mediates of T-cell signaling defects. Brit J Cancer, 92: 305-311, 2005
29. Gorak-Stolinska P, Truman JP, Kemeny DM, Noble A. Activation-induced cell death of human T-cell subsets is mediated by Fas and granzyme B but is independent of TNF-alpha. J Leuk Biol 70: 756-766, 2001.
30. Gercel-Taylor C, O'Connor SM, Lam GK, Taylor DD. Shed membrane fragment modulation of CD3-zeta during pregnancy: Link with induction of apoptosis. J Reprod Immunol, 56:29-44, 2002.
31. Lagos-Quintana, M., Rauhut, R., Lendeckel, W. & Tuschl, T. Identification of novel genes coding for small expressed RNA. Science 294:853–858, 2001.
32. Lau, N. C., Lim, L. P., Weinstein, E. G. & Bartel, D. P. An abundant class of tiny RNAs with probable regulatory roles in *Caenorhabditis elegans*. Science 294:858–862, 2001.
33. Lee R C, Ambros V. An extensive class of small RNAs in *Caenorhabditis elegans*. Science 294, 862–864, 2001.
34. Ambros V. The functions of animal microRNAs. Nature 431:350–355, 2004.
35. Lee Y, Ahn C, Han J, Choi H, Kim J, Yim J, Lee J, Provost P, Radmark O, Kim S, Kim VN. The nuclear RNase Drosha initiates microRNA processing. Nature 425:415-419, 2003.
36. Garzon R, Fabbri M, Cimmino A, Calin GA, Croce CM. MicroRNA expression and function in cancer. Trends in Mol Med, 12:580-587, 2006.
37. Hammond, S. M. MicroRNAs as oncogenes. Curr. Opin. Genet. Dev. 16, 4–9 (2006).
38. Croce CM, Calin GA. (2005). miRNAs, cancer, and stem cell division. Cell 122: 6–7.
39. Barad O, Meiri E, Avniel A, Aharonov R, Barzilai A, Bentwich I *et al*. (2004). MicroRNA expression detected by oligonucleotide microarrays: system establishment and expression profiling in human tissues. Genome Res 14: 2486–2494.
40. Cummins JM, Velculescu VE. Implications of micro-RNA profiling for cancer diagnosis. Oncogene, 25:6220-7, 2006.
41. Calin, G. A. *et al*. Frequent deletions and down-regulation of micro- RNA genes miR15 and miR16 at 13q14 in chronic lymphocytic leukemia. Proc. Natl Acad. Sci. USA 99, 15524–15529 (2002).Calin, G. A. *et al*. MicroRNA profiling reveals distinct signatures in B cell chronic lymphocytic leukemias. Proc. Natl Acad. Sci. USA 101, 11755–11760 (2004).
42. Iorio, M. V. *et al*. microRNA gene expression deregulation in human breast cancer. Cancer Res. 65, 7065–7070 (2005).
43. Ciafre, S. A. *et al*. Extensive modulation of a set of microRNAs in primary glioblastoma. Biochem. Biophys. Res. Commun. 334, 1351–1358 (2005).
44. Murakami, Y. *et al*. Comprehensive analysis of microRNA expression patterns in hepatocellular carcinoma and non-tumorous tissues. Oncogene 25, 2537–2545 (2006).
45. He, H. *et al*. The role of microRNA genes in papillary thyroid carcinoma. Proc. Natl Acad. Sci. USA 102, 19075–19080 (2005).
46. Yanaihara, N. *et al*. microRNA signature in lung cancer diagnosis and prognosis. Cancer Cell 9, 189–198 (2006).

47. Cummins, J. M. *et al*. The colorectal microRNAome. Proc. Natl Acad. Sci. USA 103, 3687–3692 (2006).
48. Roldo C, Missiaglia E, Hagan JP, Falconi M, Capelli P, Bersani S, Calin GA, Volinia S, Liu CG, Scarpa A, Croce CM. MicroRNA expression abnormalities in pancreatic endocrine and acinar tumors are associated with distinctive pathological features and clinical behavior. J. Clin. Oncol, 24:4677-4684, 2006
49. Volinia S, Calin GA, Liu CG, Ambs S, Cimmino A, Petrocca F, *et al*. A microRNA expression signature of human solid tumors define cancer gene targets. Proc. Natl Acad. Sci. USA 103:2257–2261, 2006.
50. Esquela-Kerscher A, Slack FJ. Oncomirs- microRNAs with a role in cancer. Nature Rev. Cancer 6: 259–269, 2006.
51. Bernstein E, Kim SY, Carmell MA, Murchison EP, Alcorn H, Li MZ *et al*. Dicer is essential for mouse development. Nat Genet 35:215–217, 2003.
52. Ali, I. U., Schriml, L. M. & Dean, M. Mutational spectra of PTEN/MMAC1 gene: a tumor suppressor with lipid phosphatase activity. J. Natl Cancer Inst. 91:1922–1932, 1999.
53. Iorio, M.V., *et al*. MicroRNA signatures in human ovarian cancer. *Cancer Res.* 67, 8699-8707, 2007.
54. De Cecco, L., *et al.* Gene expression profiling of advanced ovarian cancer: Characteristization of a molecular signature involving fibroblast growth factor 2. *Oncogene* 23, 8171-8183, 2004.
55. Calin, G.A. & Croce, C.M. MicroRNA signatures in human cancers. *Nature Rev Cancer* 6, 857-866, 2006.
56. Lu, J. *et al.* MicroRNA expression profiles classify human cancers. *Nature* 435, 834-838, 2005.
57. Storey and Tibshirani, 2003 J.D. Storey and R. Tibshirani, Statistical significance for genome-wide studies, *Proc. Natl. Acad. Sci. USA* 100: 9440–9445, 2003.

ATTACHMENT 1

		M1	M2	M3	M4	M5	M6	M7	M8	M9	M10	M11	M12
Position	Well	Ct (dRn)	Ct (dRn)	Ct (dRn)	Ct (dRn)	Ct (dRn)	Ct (dRn)	Ct (dRn)	Ct (dRn)	Ct (dRn)	Ct (dRn)	Ct (dRn)	Ct (dRn)
A01	let-7a	17.78	14.44	13.02	12.93	12.46	12.74	14.88	14.36	12.86	11.58	13.81	12.91
A02	miR-133b	29.20	18.54	15.23	15.48	14.07	17.10	18.04	26.96	14.65	11.99	26.34	16.25
A03	miR-122	31.81	18.67	15.77	16.13	14.08	17.32	17.06	29.35	14.99	13.09	29.39	16.26
A04	miR-20b	20.90	15.99	13.67	15.05	14.06	15.00	16.74	17.90	14.18	12.03	17.22	14.18
A05	miR-335	26.91	18.52	14.70	15.89	14.55	17.04	17.24	23.61	15.11	12.88	22.87	15.68
A06	miR-196a	25.19	17.49	15.59	16.79	14.11	16.72	18.10	21.89	14.42	12.97	21.59	15.65
A07	miR-125a-5p	16.73	13.98	12.76	13.16	12.32	12.43	13.20	13.76	12.39	11.60	14.00	12.87
A08	miR-142-5p	32.45	16.88	14.55	16.04	13.41	16.39	16.66	29.30	14.19	12.16	29.40	14.27
A09	miR-96	21.19	15.12	13.31	13.72	12.82	13.92	14.89	17.38	13.48	11.36	17.04	13.65
A10	miR-222	27.30	16.62	14.75	14.17	12.60	15.77	15.45	23.24	13.88	11.17	20.73	14.49
A11	miR-148b	19.66	14.95	13.40	13.41	12.22	13.68	15.32	16.32	12.91	11.37	15.43	13.35
A12	miR-92a	19.28	14.41	12.96	13.22	12.33	13.64	14.50	15.79	12.74	11.17	14.99	13.12
B01	miR-184	30.84	30.32	28.42	28.41	28.34	27.81	29.82	27.59	28.24	27.74	27.72	28.03
B02	miR-214	31.43	30.29	29.36	29.97	29.89	29.99	32.89	29.19	30.65	29.35	28.65	30.17
B03	miR-15a	22.06	20.39	18.87	18.85	19.13	18.17	24.68	18.53	19.04	17.96	18.19	19.00
B04	miR-18b	27.94	26.45	25.27	24.27	25.74	25.38	27.68	23.82	30.47	24.40	23.13	25.40
B05	miR-378	20.27	18.19	17.19	17.39	16.94	16.11	19.73	16.46	17.10	16.97	16.62	16.88
B06	let-7b	20.23	18.96	17.28	16.67	17.17	16.40	20.91	16.75	16.93	16.55	16.12	16.89
B07	miR-205	23.15	22.06	20.82	20.81	21.74	19.77	24.13	19.94	20.06	20.03	20.13	20.49
B08	miR-181a	20.05	18.80	17.35	16.93	18.11	16.81	22.00	16.84	16.54	16.25	16.92	17.10
B09	miR-130a	26.32	25.63	24.10	23.45	24.77	23.16	29.50	23.06	23.59	22.97	23.28	23.38
B10	miR-199a-3p	26.54	24.52	23.21	23.83	22.93	22.24	25.69	23.16	23.21	23.08	23.47	23.54
B11	miR-140-5p	24.06	22.52	20.45	20.87	20.91	19.50	25.30	20.14	20.86	20.05	20.08	20.95
B12	miR-20a	19.11	17.66	15.88	15.30	15.61	14.92	20.23	15.52	17.68	15.05	15.26	15.63
C01	miR-146b-5p	22.90	21.08	19.66	19.84	19.41	18.75	21.22	19.62	19.55	19.07	19.40	19.96
C02	miR-132	25.63	24.22	22.13	20.95	21.07	20.93	24.95	22.02	21.32	20.80	21.08	21.11
C03	miR-193b	19.71	17.86	16.93	16.70	17.23	16.43	20.73	17.09	16.55	16.40	16.56	16.86
C04	miR-183	20.36	18.07	17.05	16.85	17.00	16.07	18.27	17.04	16.56	16.36	16.62	16.73
C05	miR-34c-5p	30.18	28.90	27.74	26.82	27.83	27.49	30.13	26.84	28.86	26.77	26.30	27.71
C06	miR-30c	19.54	17.51	16.86	16.73	17.19	16.06	19.20	16.19	16.51	15.97	16.07	16.37
C07	miR-148a	19.38	17.35	16.28	15.40	15.73	15.25	31.03	15.84	15.92	15.14	15.08	15.82
C08	miR-134	32.91	30.59	29.68	30.27	30.33	29.46	30.74	29.06	30.05	29.62	26.85	30.23
C09	let-7g	19.57	17.70	16.09	15.98	16.01	15.41	19.80	15.87	16.19	15.33	15.42	16.25
C10	miR-138	30.23	28.84	27.99	27.39	28.08	27.09	31.01	27.01	27.69	26.01	25.68	27.88
C11	miR-373	31.84	31.19	29.29	29.36	30.36	30.84	32.11	28.70	30.25	29.97	28.11	31.90
C12	let-7c	23.30	22.10	21.56	20.58	21.10	19.71	23.65	20.05	21.09	19.93	19.66	20.40
D01	let-7e	18.34	16.71	15.47	15.23	15.16	14.39	17.98	14.74	15.44	14.38	14.31	15.05
D02	miR-218	24.33	22.40	21.25	21.22	20.94	19.61	25.34	20.40	20.85	20.47	21.10	21.59
D03	miR-29b	26.95	24.18	23.56	24.49	24.56	23.34	29.31	23.27	25.57	22.72	23.55	24.87
D04	miR-146a	31.95	30.68	29.17	28.71	29.55	28.27	30.42	29.02	29.81	28.40	28.52	29.27
D05	miR-212	28.19	26.04	24.99	25.45	26.25	25.98	27.72	24.80	28.27	25.78	25.06	26.15
D06	miR-135b	26.73	24.51	22.83	21.31	21.80	22.71	27.18	22.95	23.43	22.18	21.43	22.95
D07	miR-206	31.40	30.12	28.95	29.59	29.52	28.96	31.50	27.97	29.88	29.46	27.73	29.88
D08	miR-124	28.84	26.58	26.01	26.35	28.33	26.45	29.01	26.10	26.94	25.65	25.58	26.76
D09	miR-21	13.29	11.62	10.68	10.64	9.68	10.72	11.77	9.98	10.60	9.84	9.83	10.80
D10	miR-181d	22.80	21.55	20.04	20.06	20.26	19.25	24.09	19.32	19.93	19.06	19.49	19.87
D11	miR-301a	19.92	18.19	16.82	16.41	16.74	15.76	23.35	16.31	16.90	15.62	15.38	16.88
D12	miR-200c	No Ct	No Ct	No Ct	No Ct	No Ct	No Ct	No Ct	No Ct	No Ct	No Ct	No Ct	No Ct
E01	miR-100	25.51	24.48	23.52	23.28	23.40	22.08	24.25	22.74	23.69	22.76	23.13	23.46
E02	miR-10b	29.47	28.13	27.07	27.32	27.08	26.33	29.04	26.77	28.10	27.10	26.62	27.20
E03	miR-155	31.20	29.27	28.79	28.15	28.17	27.80	30.44	28.09	28.75	28.62	27.44	28.47
E04	miR-1	31.19	29.27	28.18	28.29	27.67	26.83	30.91	27.81	28.96	28.17	27.86	29.41
E05	miR-363	28.36	26.08	25.34	24.75	25.22	24.14	29.09	25.33	24.79	24.54	24.77	25.05
E06	miR-150	30.04	28.33	27.50	27.33	27.16	25.88	28.58	26.53	25.91	26.99	26.75	26.48
E07	let-7i	19.42	17.27	16.35	15.63	16.04	15.60	20.26	15.82	16.07	15.08	15.22	15.59
E08	miR-27b	18.01	15.64	14.39	14.75	14.62	14.08	16.67	14.56	14.43	14.00	14.12	14.87
E09	miR-7	18.96	16.82	15.48	15.79	15.32	14.67	17.44	15.31	16.13	15.23	15.11	16.60
E10	miR-127-5p	28.12	26.14	23.42	25.11	25.95	26.05	25.25	24.71	28.82	24.56	20.34	27.13
E11	miR-29a	20.73	19.07	17.85	17.09	17.19	16.53	22.86	16.57	17.69	17.15	16.76	17.01
E12	miR-191	16.68	14.57	14.11	13.58	13.47	12.83	14.99	13.50	13.50	13.29	13.36	13.21
F01	let-7d	20.41	18.64	17.39	16.89	17.72	16.83	21.10	17.84	17.57	16.74	16.57	16.89
F02	miR-9	23.87	21.63	20.31	20.23	19.98	19.24	21.59	20.25	21.01	19.91	20.25	20.80
F03	let-7f	24.54	22.81	21.65	22.11	20.77	20.77	23.80	20.96	24.06	21.05	20.70	22.20
F04	miR-10a	28.50	27.34	26.30	26.30	26.20	25.13	25.59	26.04	26.50	26.82	25.76	26.68
F05	miR-181b	20.02	18.24	17.09	17.24	17.47	16.35	20.18	16.61	16.75	16.57	16.82	17.01
F06	miR-15b	17.49	15.29	14.51	13.88	14.29	13.57	15.40	14.07	14.05	13.28	13.87	13.92
F07	miR-16	15.52	13.77	12.60	12.39	11.87	11.93	14.48	12.03	12.34	12.12	11.95	12.47
F08	miR-210	25.24	22.73	21.60	21.53	22.19	21.85	26.30	21.33	22.13	20.61	19.78	20.95
F09	miR-17	19.33	17.69	16.19	15.38	15.95	15.40	20.55	15.45	15.78	15.48	15.10	15.63
F10	miR-98	22.08	19.95	18.65	18.66	18.02	17.37	21.34	17.83	19.19	17.80	18.12	18.99
F11	miR-34a	23.52	22.00	20.82	19.53	20.83	19.01	25.69	19.06	20.60	18.61	18.61	19.59

F12	miR-25	17.65	15.77	14.69	14.06	14.20	13.76	15.29	14.22	14.51	13.60	14.29	14.04
G01	miR-144	35.77	34.55	32.97	32.19	No Ct	32.65	37.18	31.00	34.64	31.85	30.80	33.58
G02	miR-128	21.37	19.17	18.51	18.29	17.87	17.23	19.57	17.34	18.19	17.81	17.76	17.97
G03	miR-143	29.25	27.53	26.10	25.80	28.15	25.82	29.36	25.09	27.35	25.33	25.02	26.72
G04	miR-215	29.84	27.93	26.60	26.62	25.44	25.34	28.04	25.73	26.58	26.26	26.04	26.42
G05	miR-19a	19.52	17.32	15.88	15.35	15.81	15.32	22.24	15.61	16.00	15.08	15.21	16.12
G06	miR-193a-5p	26.35	24.89	23.74	23.48	24.07	22.73	26.53	23.34	23.11	23.42	22.06	23.73
G07	miR-18a	21.91	20.29	18.58	18.10	18.16	17.54	23.72	17.45	18.73	16.79	17.54	18.11
G08	miR-125b	20.73	19.06	19.74	18.38	18.41	17.05	17.93	17.46	18.03	17.45	18.05	18.12
G09	miR-126	20.93	19.09	17.87	18.02	17.86	16.82	20.70	17.55	17.72	17.29	17.71	17.76
G10	miR-27a	17.89	15.84	14.66	14.24	14.01	13.72	16.60	14.06	14.18	13.72	13.56	14.21
G11	miR-372	28.08	26.89	25.27	26.42	27.05	26.86	33.69	25.35	26.89	25.94	23.47	27.46
G12	miR-149	25.77	22.84	22.69	23.43	23.42	21.93	23.57	21.71	22.63	22.84	22.98	23.05
H01	miR-23b	19.15	16.58	15.56	15.63	15.81	15.42	17.36	15.33	15.50	15.20	15.33	15.79
H02	miR-203	19.91	18.64	16.90	16.56	16.28	15.75	17.26	16.67	16.82	16.34	16.54	16.71
H03	miR-32	28.17	24.55	24.78	25.21	25.53	24.34	29.12	24.18	26.17	24.44	24.66	25.90
H04	miR-181c	20.83	19.47	18.23	18.02	18.74	17.52	22.78	17.15	17.74	17.60	17.37	17.87
H05	SNORD48	26.38	24.49	23.68	23.27	23.66	22.77	27.38	22.50	24.37	22.44	21.47	22.72
H06	SNORD47	19.74	16.95	16.98	16.35	16.41	15.78	18.35	14.44	16.36	15.85	15.42	16.52
H07	SNORD44	15.99	13.64	13.15	12.88	12.55	12.46	14.03	12.37	12.78	12.40	12.17	12.50
H08	U6	21.98	18.38	19.21	19.86	19.11	19.00	23.49	17.25	19.38	18.81	16.90	17.79
H09	miRTC	22.22	18.82	18.54	19.06	19.14	18.64	23.55	19.05	19.18	19.02	18.73	18.86
H10	miRTC	22.28	18.73	18.56	18.88	19.12	18.60	23.29	18.86	19.14	18.61	19.46	19.12
H11	PPC	19.49	16.16	15.80	15.82	16.14	15.70	15.54	16.13	15.79	16.17	15.49	15.81
H12	PPC	19.40	16.23	15.75	16.08	16.20	15.77	15.79	16.18	15.93	16.34	15.75	15.80

ATTACHMENT 2

PCR Array Catalog #:		MAH-102					
				Control	Group 1	Group 2	Group 3
Position	**Mature ID**	**Accession Number**	**miRNA Catalog**	**HUMAN AB-2**	**1211463 (bladder)**	**1449338 (colon)**	**1622634 (pancreas)**
A01	let-7a	MIMAT0000062	MPH00001A	Ct (dRn)	Ct (dRn)	Ct (dRn)	Ct (dRn)
A02	miR-133b	MIMAT0000770	MPH00033A	35.50	Undetermined	22.44	19.35
A03	miR-122	MIMAT0000421	MPH00020A	33.86	Undetermined	21.4	20.14
A04	miR-20b	MIMAT0001413	MPH00105A	34.45	Undetermined	22.4	18.2
A05	miR-335	MIMAT0000765	MPH00166A	33.12	35.89	21.56	18.35
A06	miR-196a	MIMAT0000226	MPH00085A	38.25	Undetermined	22.8	20.38
A07	miR-125a-5p	MIMAT0000443	MPH00022A	34.93	38.38	21.83	19.74
A08	miR-142-5p	MIMAT0000433	MPH00043A	29.79	34.55	21.36	18.73
A09	miR-96	MIMAT0000095	MPH00479A	35.53	Undetermined	19.7	18.39
A10	miR-222	MIMAT0000279	MPH01230A	34.37	35.47	23.46	16.83
A11	miR-148b	MIMAT0000759	MPH01183A	34.15	36.84	20.9	17.53
A12	miR-92a	MIMAT0000092	MPH01375A	36.61	37.05	20.98	17.46
B01	miR-184	MIMAT0000454	MPH00070A	29.19	31.78	19.57	18.15
B02	miR-214	MIMAT0000271	MPH01223A	36.39	Undetermined	37.88	38.13
B03	miR-15a	MIMAT0000068	MPH00060A	31.35	34.58	35.41	34.88
B04	miR-18b	MIMAT0001412	MPH00076A	33.67	39.32	37.17	36.53
B05	miR-378	MIMAT0000732	MPH01284A	32.10	38.52	34.75	34.8
B06	let-7b	MIMAT0000063	MPH00002A	33.09	38.14	36.19	37.11
B07	miR-205	MIMAT0000266	MPH00100A	32.48	37.47	37.55	Undetermined
B08	miR-181a	MIMAT0000256	MPH00064A	32.53	39.54	36.41	36.36
B09	miR-130a	MIMAT0000425	MPH01165A	34.48	38.67	36.53	37.66
B10	miR-199a-3p	MIMAT0000232	MPH01212A	32.33	37.04	35.78	36.41
B11	miR-140-5p	MIMAT0000431	MPH00041A	35.71	Undetermined	Undetermined	39.31
B12	miR-20a	MIMAT0000075	MPH00104A	37.99	Undetermined	38.09	Undetermined
C01	miR-146b-5p	MIMAT0002809	MPH00048A	33.48	35.87	36.23	37.09
C02	miR-132	MIMAT0000426	MPH01167A	35.31	Undetermined	36.56	37.2
C03	miR-193b	MIMAT0002819	MPH01208A	31.86	36.01	35.56	34.51
C04	miR-183	MIMAT0000261	MPH00069A	31.39	35.85	34.93	35.67
C05	miR-34c-5p	MIMAT0000686	MPH00178A	33.49	39.66	Undetermined	Undetermined
C06	miR-30c	MIMAT0000244	MPH00152A	30.08	34.91	35.44	35.29
C07	miR-148a	MIMAT0000243	MPH01182A	34.79	Undetermined	Undetermined	Undetermined
C08	miR-134	MIMAT0000447	MPH00034A	34.34	36.75	37.15	38.68
C09	let-7g	MIMAT0000414	MPH00007A	36.06	38.68	39.47	Undetermined
C10	miR-138	MIMAT0000430	MPH00039A	Undetermined	Undetermined	Undetermined	39.21
C11	miR-373	MIMAT0000726	MPH01280A	32.74	38.17	36.34	36.2
C12	let-7c	MIMAT0000064	MPH00003A	33.26	38.96	37.83	37.57
D01	let-7e	MIMAT0000066	MPH00005A	35.89	Undetermined	39.19	Undetermined
D02	miR-218	MIMAT0000275	MPH00115A	34.52	37.93	39.35	Undetermined
D03	miR-29b	MIMAT0000100	MPH01245A	33.48	Undetermined	Undetermined	Undetermined
D04	miR-146a	MIMAT0000449	MPH00047A	35.77	Undetermined	Undetermined	39.56
D05	miR-212	MIMAT0000269	MPH00109A	35.38	Undetermined	37.57	38.73
D06	miR-135b	MIMAT0000758	MPH00036A	29.46	33.56	32.63	32.08
D07	miR-206	MIMAT0000462	MPH00101A	32.04	37.42	32.42	38.7
D08	miR-124	MIMAT0000422	MPH01157A	32.18	Undetermined	36.04	34.98
D09	miR-21	MIMAT0000076	MPH00106A	28.03	32.08	32.71	31.97
D10	miR-181d	MIMAT0002821	MPH00067A	31.46	34.45	38.19	38.94
D11	miR-301a	MIMAT0000688	MPH00144A	34.09	36.91	38.92	37.47
D12	miR-200c	MIMAT0000617	MPH01218A	33.61	35.88	37.45	36.19
E01	miR-100	MIMAT0000098	MPH00009A	33.95	35.95	34.03	36.92
E02	miR-10b	MIMAT0000254	MPH00018A	34.67	38.67	37.77	39.06
E03	miR-155	MIMAT0000646	MPH00059A	33.98	Undetermined	38.34	38.01
E04	miR-1	MIMAT0000416	MPH00019A	35.82	39.44	Undetermined	39.52
E05	miR-363	MIMAT0000707	MPH01276A	29.69	Undetermined	35.7	Undetermined
E06	miR-150	MIMAT0000451	MPH00054A	33.99	37.94	38.94	Undetermined
E07	let-7i	MIMAT0000415	MPH00008A	32.52	Undetermined	39.7	34.35
E08	miR-27b	MIMAT0000419	MPH01240A	33.31	36.95	33.42	36.57
E09	miR-7	MIMAT0000252	MPH00427A	34.55	Undetermined	Undetermined	Undetermined
E10	miR-127-5p	MIMAT0004604	MPH00025A	30.90	36.62	35.36	36.64
E11	miR-29a	MIMAT0000086	MPH01244A	32.81	Undetermined	38.49	38.89
E12	miR-191	MIMAT0000440	MPH00079A	32.70	38.08	37.57	36.85
F01	let-7d	MIMAT0000065	MPH00004A	31.55	38.35	35.18	36.28
F02	miR-9	MIMAT0000441	MPH00456A	33.51	35.41	36.42	36.45
F03	let-7f	MIMAT0000067	MPH00006A	33.08	38.8	34.89	37.28
F04	miR-10a	MIMAT0000253	MPH00017A	36.92	Undetermined	Undetermined	Undetermined
F05	miR-181b	MIMAT0000257	MPH00065A	34.35	Undetermined	37.44	38.43
F06	miR-15b	MIMAT0000417	MPH00061A	28.34	33.86	32.8	33.34
F07	miR-16	MIMAT0000069	MPH00062A	33.22	34.55	Undetermined	39.48
F08	miR-210	MIMAT0000267	MPH00107A	31.59	34.27	35.81	36.38
F09	miR-17	MIMAT0000070	MPH00063A	27.07	31.96	30.31	31.65
F10	miR-98	MIMAT0000096	MPH00480A	31.49	34.95	33.35	34.63
F11	miR-34a	MIMAT0000255	MPH00176A	36.27	Undetermined	Undetermined	Undetermined
F12	miR-25	MIMAT0000081	MPH01235A	33.06	36.75	35.4	37.82
G01	miR-144	MIMAT0000436	MPH01178A	32.07	33.65	34.77	37.84
G02	miR-128	MIMAT0000424	MPH00026A	37.59	Undetermined	Undetermined	Undetermined
G03	miR-143	MIMAT0000435	MPH01177A	34.29	39.33	38.83	Undetermined
G04	miR-215	MIMAT0000272	MPH00111A	33.25	37.28	33.24	37.79
G05	miR-19a	MIMAT0000073	MPH01214A	35.15	Undetermined	38.14	Undetermined
G06	miR-193a-5p	MIMAT0004614	MPH00081A	32.36	38.39	33.91	36.64
G07	miR-18a	MIMAT0000072	MPH00075A	30.36	34.2	33.94	32.81
G08	miR-125b	MIMAT0000423	MPH00023A	32.58	36.22	36.56	36.16
G09	miR-126	MIMAT0000445	MPH01161A	30.75	35.39	31.16	34.64
G10	miR-27a	MIMAT0000084	MPH01239A	31.99	39.65	34.38	Undetermined
G11	miR-372	MIMAT0000724	MPH00187A	32.48	38.7	37.57	38.49

G12	miR-149	MIMAT0000450	MPH00053A	29.42	33.63	34.33	31.51
H01	miR-23b	MIMAT0000418	MPH01233A	33.04	36.89	35.92	36.02
H02	miR-203	MIMAT0000264	MPH00098A	32.64	36.3	37.47	Undetermined
H03	miR-32	MIMAT0000090	MPH00156A	32.34	35.51	34.37	38.78
H04	miR-181c	MIMAT0000258	MPH00066A	36.24	Undetermined	Undetermined	Undetermined
H05	SNORD48	NR_002745	MPH01657A	30.43	31.65	30.36	31.16
H06	SNORD47	NR_002746	MPH01660A	28.60	33.58	32.91	34.74
H07	SNORD44	NR_002750	MPH01658A	34.69	39.9	39.16	Undetermined
H08	RNU6-2	NR_002752	MPH01653A	35.10	Undetermined	Undetermined	Undetermined
H09	miRTC	SA_miRNA_005	MPH01656A	30.32	37.22	34.52	32.97
H10	miRTC	SA_miRNA_005	MPH01656A	18.47	23.35	18.57	21.44
H11	PPC	SA_00104	PPX63339A	18.41	23.04	18.62	20.97
H12	PPC	SA_00104	PPX63339A	16.64	17.28	17.92	17.23
				16.67	17.44	17.94	16.89

ATTACHMENT 3a

	Symbol	Description	Control	Exo-Treated
A01	ADA	Adenosine deaminase	22.26	18.59
A02	AICDA	Activation-induced cytidine deaminase	35	19.52
A03	APC	Adenomatous polyposis coli	29.04	17.34
A04	BCL2	B-cell CLL/lymphoma 2	26.64	18.84
A05	BLM	Bloom syndrome, RecQ helicase-like	25.9	20.27
A06	BLNK	B-cell linker	29.62	18.43
A07	CCL3	Chemokine (C-C motif) ligand 3	20.25	18.2
A08	CCR1	Chemokine (C-C motif) receptor 1	22.74	17.38
A09	CCR2	Chemokine (C-C motif) receptor 2	34.57	20.14
A10	CCR3	Chemokine (C-C motif) receptor 3	30.74	19.21
A11	CCR4	Chemokine (C-C motif) receptor 4	33.39	22.08
A12	CCR5	Chemokine (C-C motif) receptor 5	32.92	17.54
B01	CD1D	CD1d molecule	27.58	35
B02	CD2	CD2 molecule	30.68	35
B03	CD27	CD27 molecule	32.64	35
B04	CD274	CD274 molecule	30.97	35
B05	CD276	CD276 molecule	26.49	35
B06	CD28	CD28 molecule	22.36	35
B07	CD3D	CD3d molecule, delta (CD3-TCR complex)	35	35
B08	CD3E	CD3e molecule, epsilon (CD3-TCR complex)	25.73	35
B09	CD3G	CD3g molecule, gamma (CD3-TCR complex)	33.33	35
B10	CD4	CD4 molecule	31.43	35
B11	CD40	CD40 molecule, TNF receptor superfamily member 5	29.23	35
B12	CD40LG	CD40 ligand	32.39	30.63
C01	CD47	CD47 molecule	22.98	35
C02	CD5	CD5 molecule	35	35
C03	CD7	CD7 molecule	30.83	34.36
C04	CD80	CD80 molecule	33.14	35
C05	CD81	CD81 molecule	23.04	35
C06	CD86	CD86 molecule	27.56	35
C07	CD8A	CD8a molecule	32.92	35
C08	CD8B	CD8b molecule	35	35
C09	CSF2	Colony stimulating factor 2 (granulocyte-macrophage)	29.81	32.71
C10	CX3CL1	Chemokine (C-X3-C motif) ligand 1	33.8	32.65
C11	CXCR3	Chemokine (C-X-C motif) receptor 3	27.67	34.49
C12	CXCR4	Chemokine (C-X-C motif) receptor 4	35	35
D01	CXCR5	Chemokine (C-X-C motif) receptor 5	32.24	35
D02	DPP4	Dipeptidyl-peptidase 4	32.49	35
D03	EGR1	Early growth response 1	29.28	35
D04	FAS	Fas (TNF receptor superfamily, member 6)	25.55	35
D05	FASLG	Fas ligand (TNF superfamily, member 6)	31.91	35
D06	FOXP3	Forkhead box P3	28.83	34.15
D07	ICOSLG	Inducible T-cell co-stimulator ligand	27.24	35
D08	IFNG	Interferon, gamma	32.47	35
D09	IL10	Interleukin 10	27.4	35
D10	IL11	Interleukin 11	33.88	35
D11	IL12A	Interleukin 12A (natural killer cell stimulatory factor 1, cyto	26.47	35

D12	IL12B	Interleukin 12B (natural killer cell stimulatory factor 2, cyto	35	35
E01	IL12RB1	Interleukin 12 receptor, beta 1	25.13	33.29
E02	IL12RB2	Interleukin 12 receptor, beta 2	28.17	35
E03	IL13	Interleukin 13	30.04	33.41
E04	IL15	Interleukin 15	27.78	35
E05	IL18	Interleukin 18 (interferon-gamma-inducing factor)	30.9	34.26
E06	IL18R1	Interleukin 18 receptor 1	32.58	35
E07	IL1B	Interleukin 1, beta	33.33	35
E08	IL2	Interleukin 2	35	34.79
E09	IL2RA	Interleukin 2 receptor, alpha	35	35
E10	IL3	Interleukin 3 (colony-stimulating factor, multiple)	32.12	35
E11	IL4	Interleukin 4	33.1	35
E12	IL4R	Interleukin 4 receptor	27.09	35
F01	IL5	Interleukin 5 (colony-stimulating factor, eosinophil)	32.61	35
F02	IL6	Interleukin 6 (interferon, beta 2)	34.2	35
F03	IL7	Interleukin 7	35	35
F04	IL8	Interleukin 8	29.15	35
F05	IRF4	Interferon regulatory factor 4	20.03	35
F06	LAG3	Lymphocyte-activation gene 3	35	35
F07	LCK	Lymphocyte-specific protein tyrosine kinase	31.16	35
F08	MAP3K7	Mitogen-activated protein kinase kinase kinase 7	24.42	35
F09	MICB	MHC class I polypeptide-related sequence B	24.1	33.52
F10	MS4A1	Membrane-spanning 4-domains, subfamily A, member 1	35	35
F11	NCK1	NCK adaptor protein 1	24.92	35
F12	NOS2	Nitric oxide synthase 2, inducible	33.92	35
G01	PTPRC	Protein tyrosine phosphatase, receptor type, C	30.72	35
G02	RAG1	Recombination activating gene 1	34.2	35
G03	RIPK2	Receptor-interacting serine-threonine kinase 2	26.42	35
G04	SOCS1	Suppressor of cytokine signaling 1	27.94	35
G05	TGFB1	Transforming growth factor, beta 1	20.78	35
G06	TLR1	Toll-like receptor 1	32.47	35
G07	TLR2	Toll-like receptor 2	35	35
G08	TLR4	Toll-like receptor 4	26.03	35
G09	TLR6	Toll-like receptor 6	29.3	35
G10	TLR9	Toll-like receptor 9	33.12	35
G11	TNFSF14	Tumor necrosis factor (ligand) superfamily, member 14	34.71	34.51
G12	VAV1	Vav 1 guanine nucleotide exchange factor	22.33	35
H01	ACTB	Actin, beta	18.69	35
H02	B2M	Beta-2-microglobulin	19.19	32.5
H03	GAPDH	Glyceraldehyde-3-phosphate dehydrogenase	19.81	32.64
H04	HPRT1	Hypoxanthine phosphoribosyltransferase 1	23.65	35
H05	RPLP0	Ribosomal protein, large, P0	16.82	29.13
H06	HGDC	Human Genomic DNA Contamination	35	35
H07	RTC	Reverse Transcription Control	20.97	20.15
H08	RTC	Reverse Transcription Control	20.91	19.33
H09	RTC	Reverse Transcription Control	20.97	19.92
H10	PPC	Positive PCR Control	16.88	16.81
H11	PPC	Positive PCR Control	16.81	16.61

H12	PPC	Positive PCR Control	16.89	16.72

	A	B	C	D	E	F
1	**SAMPLE**	**IL-4 rel exp**	**IL-6 rel exp**	**IL-10 rel exp**	**IgGH rel exp**	
2	C5h RA-1 alone	1.69	1.21	147	2500	
3	T5h (RA1+ exo)	1.22	2.73	1652		
4	T5h (+ IL-4)	1	1.92	427.6		
5	T5h (+ CD40L)	1.52	1.79	263.2		
6	T5h (ILCD)**off	1000	2000	27.8		
7	T5h (ALL)	2.71	9	1795.3	8.33	
8	C16h RA1 alone	1.82	1.93	1016.9		
9	T16h (RA1 + exo)	2.08	1.66	1509.7		
10	T16h (+ IL-4)	2	1.28	464.6		
11	T16h (+ CD40L)	2.37	2.85	1287		
12	T16h (ILCD)	3.16	1.46	96.3	16.9	
13	T16h (ALL)	1.65	3.58	2005	12.3	
14						
15	C5h H929 alone	6653	2402	4.69	102126	
16	T5h (H929 + exo)	596	243.9	4.32	4451.3	
17	T5h (+ IL-4)	3956	1596	2.68	97289.7	
18	T5h (+ CD40L)	855	421.6	1.34	11505.2	
19	T5h (ILCD)	8902.5	5000	65.8		
20	T5h (ALL)	43.1	54.2	13.5	4124	
21	C16h H929 alone	3350	1782.9	1.93	106463	
22	T16h (H929 + exo)	1.14	1.47	600	40.5	
23	T16h (+ IL-4)	13124.7	2665.1	7.57	207104.5	
24	T16h (+ CD40L)	1000	393	2.09	12077.2	
25	T16h (ILCD)	5792.6	10226.3	93.7		
26	T16h (ALL)	2.64	1.4	533.7	148.1	

ATTACHMENT 3b RA-1

	G	H	I	J
1	**SAMPLE**	**RAG1 rel exp**	**RAG2 rel exp**	**AID rel exp**
2	C5h RA-1 alone	25.6	6.25	3.13
3	T5h (RA1+ exo)			2.28
4	T5h (+ IL-4)			2
5	T5h (+ CD40L)			1.85
6	T5h (ILCD)**off	1000	3333	
7	T5h (ALL)	1.13	12.2	9.92
8	C16h RA1 alone			3.44
9	T16h (RA1 + exo)			4.34
10	T16h (+ IL-4)			4.17
11	T16h (+ CD40L)			3.22
12	T16h (ILCD)	1.43		
13	T16h (ALL)	2.77	9.09	2.55
14				
15	C5h H929 alone	6653.9	6653.6	102126
16	T5h (H929 + exo)	3061.5	1261.2	1000
17	T5h (+ IL-4)	3125.8	4576.4	97289.7
18	T5h (+ CD40L)	560.3	1000	8902.5
19	T5h (ILCD)			
20	T5h (ALL)	809	3565.8	1488.9
21	C16h H929 alone	2352.5	3565.8	66913.1
22	T16h (H929 + exo)	13.3	16.6	27.5
23	T16h (+ IL-4)	5673.4	8719.3	829521.6
24	T16h (+ CD40L)	292	364.6	178.5
25	T16h (ILCD)			
26	T16h (ALL)	19.97	216.7	1.